Efficient Deployment of UAVs for Search and Rescue Operations in Disaster Recovery Management

Thesis

Aalborg University

Department of Electronic Systems
www.es.aau.dk

Title

Efficient Deployment of UAVs for Search and Rescue Operations in Disaster Recovery Management

Project type

Thesis

Project period

September 2023 - March 2024

Participant

Pushpa Neupane
pneupa21@student.aau.dk

Supervisor

Rasmus Løvenstein Olsen
rlo@es.aau.dk

Number of pages: 66
Date of completion: March 11, 2024

Abstract

Recently, Unmanned Aerial vehicles (UAVs) have gained significant attention in many fields due to their ease of deployment, flexibility, and affordability. They are widely used for disaster management, surveillance, border monitoring, battlefield monitoring, data collection, crop monitoring, communication services, emergency aid, etc. This thesis primarily investigates the role of UAVs in supporting search and rescue teams in a disaster, intending to facilitate rescue operations and provide services to victims using minimal resources. In this context, they provide real-time information that can aid decision-making. UAVs in disaster management can decrease response time, cover a wide area, and analyze the situation quickly. To provide complete rescue operations with the optimal number of UAVs and minimum energy consumption, we test four different algorithms for UAV trajectory planning, namely, Randomized Coverage Iteration (RCI), Intelligent Randomized Coverage Iteration (IRCI), scan movement, and nearest movement in the simulation environment. The performance of these algorithms is evaluated for the four different environments in terms of the number of UAVs required to cover the whole area, average total distance travelled, average energy consumption, and number of configurations. Simulation results indicate that the scan algorithm requires the least number of UAVs for coverage in all environments compared to other algorithms. Moreover, we analyze the impact of various height bounds on the coverage radius and the required number of UAVs to cover the entire area in different environments.

Nomenclature

Abbreviations

UAV	Unmanned Aerial Vehicle
ABS	Aerial Base Station
BS	Base Station
A2G	Air-to-Ground
A2A	Air-to-Air
LoS	Line-of-Sight
NLoS	Non Line-of-Sight
QoS	Quality-of-Service
LAPs	Low Altitude Platforms
HAPs	High Altitude Platforms
AP	Altitude Platform
RCI	Randomized Coverage Iteration
IRCI	Intelligent Randomized Coverage Iteration

Preface

Harvard referencing style is followed for referencing of research papers. Bibliography can be found at the end of this work. Figures, tables, and equations are inserted and enumerated according to the chapters. A list of abbreviations is provided in the beginning of the work and they are called in thesis work to avoid repetition of long words. This thesis work is carried out using certain software and tools including Python, Powerpoint, Draw.io, Adobe Illustrator, and Overleaf.

Thanks to my respected supervisor Rasmus Løvenstein Olsen for insightful feedback, the quality of my research and work have undergone significant improvement, which helped me to elevate the standard of work.

Contents

Introduction 1

1.1 Overview

This chapter provides the background and introduction of Unmanned Aerial Vehicle (UAV). It provides comprehensive insights into how UAVs can be used in different sectors and how the advancement of UAV technology makes effective disaster management and rescue operations possible with the incorporation of UAVs. It also summarizes the destruction and losses around the world due to natural disasters.

1.2 Background and Introduction

UAV also known as a drone, is an aerial vehicle with the capability of flying without any pilot onboard. It can be either operated using a computer or remotely controlled by the human operator. Nowadays, UAVs are getting a lot of attention due to their versatility, flexibility and affordability. UAVs are widely utilized in military, agricultural, and disaster relief applications due to their low cost, freedom from terrain constraints, and rapid coverage [Mozaffari et al., 2019; Elmeseiry et al., 2021]. Fig. 1.1 provides a glance on the applications of UAVs.

In the military, one of the most important roles of UAVs is surveillance and reconnaissance. UAVs equipped with high-resolution cameras and advanced sensors can provide real-time information on the movements of enemies, positions, and activities. UAVs used in surveillance have the capabilities to improve battle situational awareness, assist in the detection of possible threats and plan effective military plans. UAVs can be essential assets in urban warfare settings where the environment is challenging and unpredictable, supporting ground soldiers in navigating and comprehending the battlefield from above.

In agriculture, UAVs can be used for a variety of operations such as crop mapping, inspection of soil, watering, and pest management. UAVs can quickly and efficiently cover wide areas of land, allow farmers to collect data and monitor crops more efficiently. This can aid in the early detection of problems, resulting in more rapid and effective actions. UAVs can also be used for livestock management. They can assist ranchers in providing a real-time view of the livestock for better livestock management and monitoring. Thermal sensors mounted to UAVs are also utilized for nighttime observation of livestock and real-time identification of problems.

In the case of disaster management and relief, situation assessment can be remotely done by using UAVs, location mapping, providing emergency aid, extinguishing fires, etc. In this context, it helps in providing real-time information which can aid in decision-making. UAVs in disaster management can decrease response time, cover wide distances, and analyze the situation quickly.

Furthermore, UAVs can also be used in wireless networks to enhance coverage and connectivity. In UAV-assisted wireless networks, UAVs have several potentials as shown in Fig. 1.2. UAVs have the potential to provide Line-of-Sight (LoS) communication links which results in significant enhancement of coverage, capacity, delay performance of conventional wireless network [Munawar et al., 2022]. UAVs have the ability to provide additional capacity because of their mobility and communication capabilities, which can help to reduce network congestion in locations with a high density or in events that are particularly crowded. The traffic that is being carried by the ground network might be offloaded to them by acting as aerial relays or Aerial Base Station (ABS) [Sharafeddine and Islambouli, 2019]. In instances such as emergencies, disaster recovery, or events that need quick deployment of communication infrastructure, UAVs can be utilized to build temporary communication links. In addition, they have the capability to expand wireless coverage to locations where the existing infrastructure is either damaged or insufficient [Saif et al., 2021]. This makes it easier for vital operations and services to communicate in a timely and efficient manner. However, there are certain challenges associated with UAV-assisted networks as shown in Fig. 1.2, such as 3d optimal deployment, flight time issues due to energy limitations, security, and privacy concerns, etc [Mohsan et al., 2023].

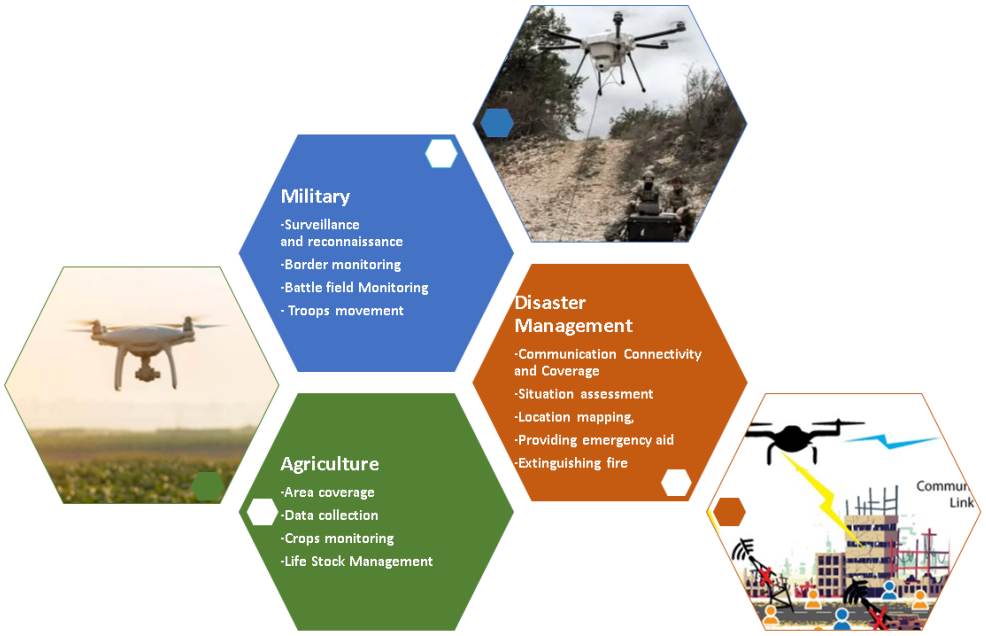

Figure 1.1. UAV Applications.

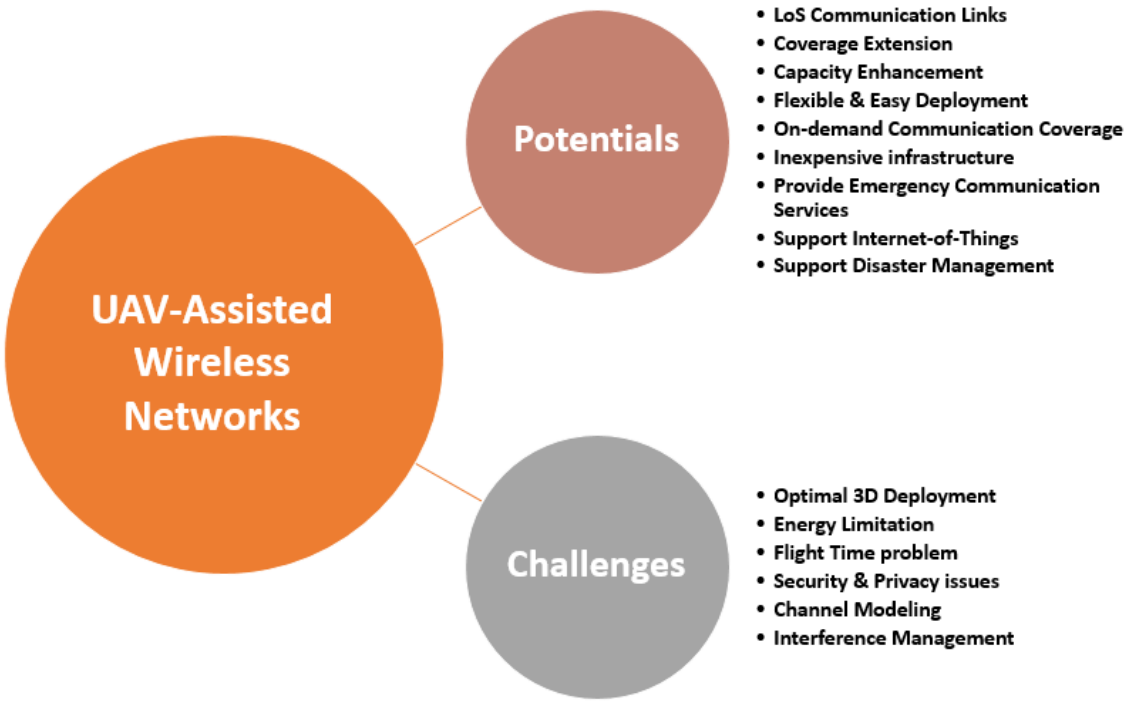

Figure 1.2. Potentials and challenges of UAV-assisted wireless networks.

In natural disaster scenarios, such as earthquakes, heavy rains, tsunamis, floods, and landslides, a significant challenge arises from the failure of communication infrastructure, which consequently affects the efficacy of response efforts. This frequently results in a large number of victims being entrapped. In the case of man-made disasters, such as terrorist attacks and hostage situations, similar situations have been observed. The continuous climate change phenomenon is projected to increase every year in a greater number with high intensity. The number of disaster events recorded across the world is shown in Fig. 1.3. According to these statistics, in 2022, the global record of natural disaster events hit 421 incidents, increasing over the previous year's stated count of 406 [Salas, 2023].

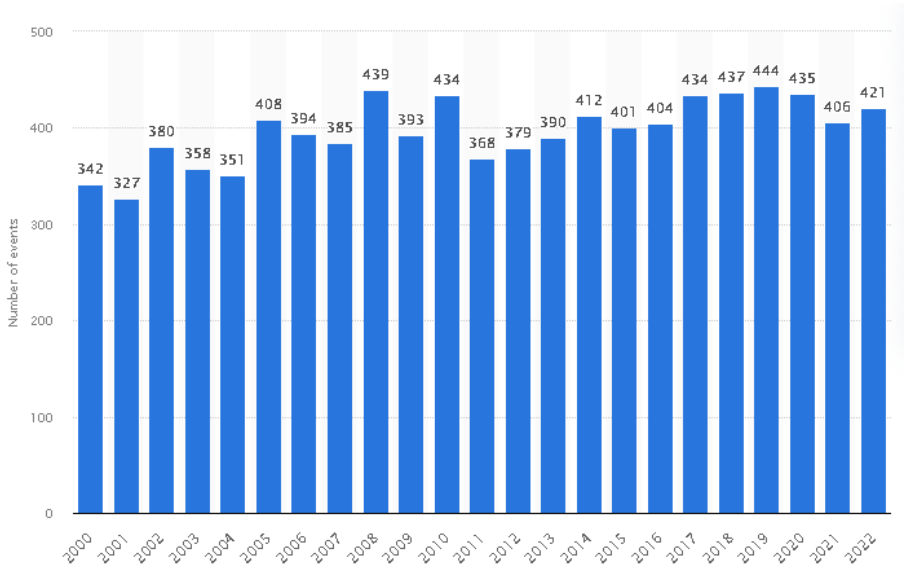

Figure 1.3. The number of disasters recorded around the world from the year 2000 to 2022.

In the year 2022, the Asian Pacific area saw the most significant incidence of natural catastrophes [Ahmed, 2023]. The adverse effects of natural disasters on individuals and nations are substantial due to their destructive nature. In 2023, the number of fatalities from natural calamities exceeded 90,000 individuals, and the global economic damage from natural catastrophes has been estimated to be 380 billion U.S. dollars [Salas, 2024a,b]. During these events, damage to infrastructure, power outages, and overloaded networks cause conventional communication technologies to fail, highlighting the need for promising alternative networks. Hence, implementing robust and self-sustainable networks is necessary to manage search and rescue operations effectively.

In this regard, UAVs offer a potentially effective way to tackle these problems. They provide a novel approach to disaster management by providing a quick and adaptable way to establish communication networks in areas devastated by disasters. In addition, UAVs can facilitate rescue teams in providing essential supplies like first aid kits and food to the victims. UAV-enabled network can be deployed in disaster-struck areas to monitor the affected zone to enable rescue workers to search and locate people or animals who are in need. Recently, there has been an increasing consideration of UAV-enabled networks, which have shown the ability to quickly establish wireless networks with large coverage. However, the limited flight time of the UAV poses certain difficulties for the low-cost deployment of emergency communication through UAV networks, as it results in reduced network lifetime and unstable network coverage which can significantly impact disaster management and rescue activities. Moreover, finding the optimal number of UAVs that are required to cover the complete target area is important for the efficient use of resources. In this work, the efficient UAV movement approach is developed to ensure the complete coverage of disaster-struck areas with efficient use of resources. In addition, the UAV energy consumption is modeled so that the energy-efficient UAV-enabled network can be established.

1.3 Problem Statement

Disaster events cause the destruction of roads, communication networks, and other infrastructure and restrict access to the disaster area. Due to the unavailability of communication services, obtaining the information of victims such as their location, number of victims, etc, is difficult and the destruction of roads makes it difficult to deliver essential supplies like first aid kits and food to the victims. **Hence, the problem investigated is:**

- **How to implement quick and robust communication service with efficient resource management to effectively perform and manage rescue operations?**

1.4 Aim & Objectives

The main aim of this work is to focus on the deployment and implementation of UAVs in disaster scenarios to enable rescue operations for providing rescue services to the victims.

The main objectives of this work are to:

- To develop an efficient movement strategy of UAVs to cover the complete target area.
- To find the optimal number of UAVs required to provide complete coverage of the target area.
- To investigate and compare different movement schemes of UAVs for ensuring complete coverage.
- To model the UAV energy consumption patterns to provide energy-efficient movement planning of UAVs.
- To investigate the completion time of rescue operations under different deployment strategies.

1.5 Thesis Structure

Fig. 1.4 shows the structure of this thesis. The thesis is composed of the following chapters:

- Chapter 1 provides insight into the overview of disaster scenarios and the importance of UAV-enabled networks in disaster events with associated challenges.
- Chapter 2 discussed the existing work in the literature on UAV-assisted communication for disaster management.
- Chapter 3 provides an outline of the assumptions guiding our study. Formulates the problem to be addressed. Different algorithms for UAVs deployment.
- Chapter 4 shows how performance is evaluated. Show the performance of all schemes, compare results and discuss findings.
- Chapter 5 summarizes and highlights the main results.

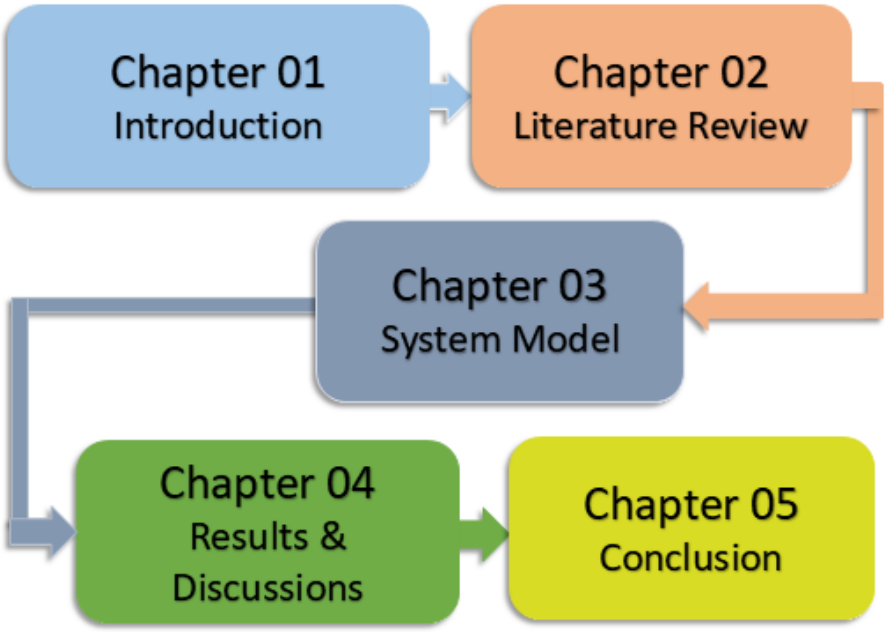

Figure 1.4. Thesis structure.

Literature Review 2

2.1 Overview

This chapter provides the overview and state-of-the-art related to UAV technology. The important role of UAVs in disasters, particularly in the context of UAVs deployment for coverage, is comprehensively explored. In addition, various works on UAV power consumption are discussed.

2.2 Diverse Roles of UAVs in Disaster

In disaster secarios, UAVs facilitate disaster management and rescue efforts in many ways. UAVs are crucial in performing prompt and efficient aerial surveys as they can provide aerial images and immediate data to facilitate efficient evaluation of the extent of damage. UAVs capabilities enables more effective collaboration among rescue team personnel in addition to prioritizing rescue efforts based on imaginary data collected through UAVs. UAVs with advanced sensors, such thermal imaging, make it possible to identify victims in dangerous or difficult-to-reach areas. Additionally, UAVs are utilized for the distribution of supplies and logistics to remote locations, guaranteeing the prompt delivery of vital aid like food, medication, and medical supplies [Khan et al., 2022]. Mapping and Geographic Information Systems (GIS) capabilities of UAVs are helpful in creating comprehensive maps of disaster-affected areas, which aid in the evaluation of infrastructure damage, resource distribution, and general situational awareness [Mavroulis et al., 2019].

Disasters often lead to serious disruptions to communication services due to destruction of communication infrastructures. UAVs play a significant role for providing wireless communication in disaster scenarios due to their ease of deployment. Particularly, UAVs as Aerial Based Stations (ABSs) are used for a variety of applications including traffic offloading from congested conventional base stations or providing wireless connectivity service in emergency scenarios such as disaster scenes or remote areas when the traditional Base Stations (BS) are difficult to deploy [Kishk et al., 2020]. The key aspects of ABS are shown in Fig. 2.1. ABSs have flexible 3D deployment which implies that they can be quickly and easily deployed in any location due to their mobility, coverage and Quality-of-Service (QoS) of on-ground users can be significantly enhanced [Bose et al., 2022]. However, they are short-term because of their battery limitation. Disasters frequently result in the destruction of traditional ground base stations, causing the network to become paralyzed. In such situations, determining how to quickly restore the network can be difficult. A fully operational communication network is critical in disaster situations where the ground infrastructure is completely or partially damaged to coordinate relief activities

and save lives. UAVs have the potential to assist disaster-stricken communities in rapidly and effectively restoring connectivity. The use of UAVs as ABSs in disaster scenarios contributes to a significant change in emergency communication networks [Zhao et al., 2019]. In contrast to traditional infrastructure, UAVs have flexibility which allows them to traverse difficult terrain and reach isolated regions where constructing ground-based communication infrastructure would be impracticable or time-consuming.

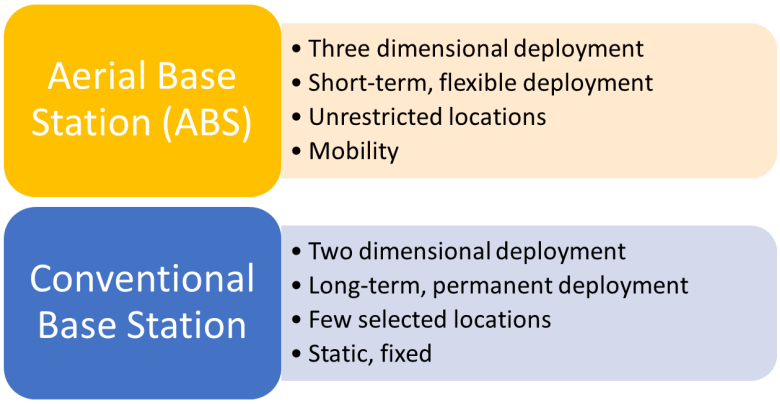

Figure 2.1. ABS vs conventional base station.

2.3 UAVs Deployment

The optimal deployment of UAVs in the target area to get optimal coverage and service quality for the ground users is challenging. Authors in [Al-Hourani et al., 2014b] optimally deploy the UAV by optimizing the altitude of a single UAV to maximize the coverage region. The work in [Mozaffari et al., 2015] expanded the scenario to include two UAVs and analyzed the influence of altitude on transmission power, taking into account the interference that could occur between them. The overview of state-of-the-work on UAV-assisted network applications and classifications is provided in [Li and Savkin, 2021]. This review also includes the analysis of the common challenges in UAV control, navigation, and deployment, and research open challenges and future directions are identified. The ABS deployment problem is addressed and investigated in the [Viet and Romero, 2022], as well as the limitations and challenges involved with it. This work also discusses the concept of adaptable placement and several techniques to address deployment problems in 2D and 3D areas. To maximize coverage, authors in [Bor-Yaliniz et al., 2016; Alzenad et al., 2017] evaluated the optimal placement of a single UAV in three-dimensional space. The work in [Wang et al., 2018] presented a traffic-aware adaptive UAV deployment scheme in which the UAV positioned at the center of the cell adjusted its distance and direction of flight in response to the Poisson-distributed mobile users present in the target cell. The optimal deployment of multiple UAVs is more challenging. In [Mozaffari et al., 2016], an efficient deployment technique based on circular packing theory is proposed for the deployment of multiple UAVs, resulting in maximal coverage in which each UAV utilizes the least amount of transmit power. The work in [Majeed et al., 2022] proposed a decision-making approach for cellular networks to use UAVs to get an effective coverage area. The approach provides a dynamic reconfiguration of nodes in the network based on UAVs

to meet the network's desired criteria. Authors in [Kalantari et al., 2016] designed a particle swarm optimization-based heuristic algorithm that calculates the least number of UAVs and their positions to serve all users in a specific region with varying user densities. Authors in [Kabashkin, 2023] presented a model for measuring sensor service availability in a wireless network with ABS placement, with a focus on the employment of UAVs in real-world settings. This model includes UAV-assisted mobile edge computing with ABS placement and a UAV energy restoration ground station. The work in [Masroor et al., 2021] focused on strategically deploying UAVs in destroyed infrastructures to provide the necessary requirement for communication as well as assistance services in emergency scenarios. The study formulates as an integer linear optimization problem a multi-objective problem including UAV placement, user-UAV communication, distance, and cost. To tackle this, a high-complexity branching and bound algorithm is introduced, along with a low-complexity heuristic for efficient goal achievement. Table 2.1 summarized the recent related work. It is observed that different techniques have been used for UAVs deployment focusing on diverse UAVs use-cases.

2.4 Path loss Modeling in UAV Networks

Path loss modeling is an important factor aspect in designing and optimizing wireless communication networks. In case of disaster recovery and management, UAVs have to fly over diverse environments including urban landscapes and open fields. These diverse environments affect communication links and impose certain challenges such as signal attenuation, blockage of LOS links, multipath fading, and penetration losses [Maxama and Markus, 2018]. Signal losses increase with the increase in path loss due to the increased distance between transmitting and receiving devices for any given environment. In the case of a hilly or irregular terrain environment, path loss is more as compared to free space. Different environments give different values of path loss exponent [Naseem et al., 2018]. Hence, it is important to model the path loss. The path loss models aid in the prediction of signal strength attenuation during the propagation of communication signals from the UAV to the BS or between UAVs. Signal propagation from UAV to ground user is referred to as Air-to-Ground (A2G) path loss and signal propagation between UAVs is referred to as Air-to-Air (A2A) path loss [Moraitis et al., 2023]. UAVs equipped with communication interfaces are also referred as Aerial Platforms (AP). Depending on the altitude of UAVs, these APs can be High Altitude Platforms (HAPs) or Low Altitude Platforms (LAPs). There are certain factors that significantly contribute to path loss in the case of UAV-assisted networks. These factors include UAV altitude and trajectory, frequency selection, multipath fading, different environments, etc. Table 2.2 summarized the some path loss models. The statistical models in [Pang et al., 2022] are proposed to predict the LOS A2G path that is appropriate for various altitudes and frequencies, with the consideration of various factors such as transceiver altitude, building height, building width, building location, and the Fresnel zone. Other models include a modified two-ray planar reflection A2G path loss model is proposed based on elevation angle (EA) with a variable reflection coefficient for the A2G channel. As a result of the influence of curved-earth approximation, the authors in [Matolak and Sun, 2016] provided a two-segment path-loss model incorporating Rician fading. Authors in [Athanasiadou and Tsoulos, 2019] investigate the path loss characteristics of the A2G channels for different altitudes of UAVs.

Table 2.1. Summary of existing work.

Ref.	**Number of UAVs**	**Technique**	**Objective Function**	**Model Scenario**
[Wu et al., 2023]	Multiple	Distance-based location selection + Mixed-integer linear program	To maximize the traffic flow from a any source to a destination node	UAV-assisted Wireless network
[Sami et al., 2023]	Multiple	K-means + Evolutionary memetic based algorithm	To support vehicular fog cluster formation and service placement	UAV-enabled Vehicular communication
[Kirubakaran and Hosek, 2023]	Multiple	Genetic algorithm	To ensure complete user coverage and permanent connections	Disaster
[Lei et al., 2023]	Multiple	Stackelberg game	to efficiently deploy limited UAVs to patrol on borders	Military
[Liu et al., 2023]	Multiple	UAV-BS deplomment algorithm	To provide on-demand wireless coverage with minimum UAVs	UAV-assisted cellular network
[Su et al., 2023]	Single & Multiple	Quasi-convex optimization	To maximize system capacity	UAV-assisted IoV (Internet-of-Vehicle) communication environment
[Bi et al., 2023]	Single	Gibbs sampling integrated with block coordinate descent	To jointly optimize of 3D deployment and resource allocation	UAV-assisted communication & localization
[Zhu and Zhou, 2023]	Single	Greedy heuristic & Particle swarm optimizer	To maximize total weighted target coverage	UAV-enabled sensor network
[Huang and Savkin, 2022]	Multiple	Decentralized deployment algorithm	To provide the optimal coverage	Disaster
[Sabzehali et al., 2022]	Multiple	Graph theory	To ensure backhaul connectivity with minimum UAVs	Remote area
[Liu et al., 2022]	Single	Proximal stochastic gradient descent based algorithm	To improve the Quality-of-Service (QoS)	UAV-assisted cellular network
[Seraj et al., 2022]	Multiple	Multi-step Adaptive Extended Kalman Filter + Wildfire propagation mathematical model	To enable accurate, online wildfire coverage and tracking	Wildfires

Authors in [Odesanya et al., 2023] proposed a hybrid approach for path loss prediction by coupling strengths of machine learning techniques and empirical models. It is important to note that statistical models are preferable because machine learning-based methods have limitations in the context of huge data requirements, optimization of parameters, and generalization.

Table 2.2. Summary of A2G path loss models.

Ref.	**Model**	**Description**
[Pang et al., 2022; Khawaja et al., 2020]	Statistical propagation models	Used to model A2G path loss in urban environments
[Ranchagoda et al., 2021]	Elevation-angle based two-ray model	Used to model the A2G path loss based on elevation angle.
[Bolli, 2020; Sun et al., 2022]	Path Loss Model Based on Environmental Variables	Used to model the A2G path loss based on environmental variables for air-to-ground communication.
[Odesanya et al., 2023]	Hybrid Path Loss Prediction Model	Used to predict path loss based on artificial intelligence and empirical models.
[Al-Hourani et al., 2014b]	Statistical Path Loss Model	Used to model A2G path loss over urban environment.

2.5 UAVs Power Consumption

In order to fully realize the potential of UAVs for providing wireless communication services, a number of challenges and technical issues must be addressed, including privacy and public safety concerns, regulatory and standardization issues, limited battery capacity, energy consumption, and so on [Mohsan et al., 2023]. One of the most concerning among these challenges is the energy consumption of UAVs. This is due to the low battery capacity of UAVs, which limits the maximum time the UAV can fly to give coverage to ground users. UAVs with different designed models have different capabilities like battery energy, flight time, hovering time, payload, etc. Table 2.3 provides the capabilities of different models of UAVs obtained from manufacturer website [Dji, 2024]. It can be seen that different models of UAVs have different specifications. The battery energy of all these models is calculated from $Battery\ Energy = Capacity \times Voltage$ using capacity in mAh and voltage in V from the manufacturer's website. Most of these parameters are measured in windless environments. These characteristics do not accurately reflect the actual operations of UAVs in the real world because, in the real world, UAVs have to experience dynamic weather conditions.

It is vital to consider the power consumption models to project and optimize the power consumption of UAVs to address this issue. There have been several research carried out in order to construct comprehensive power consumption models for UAVs. These models are based on analysis of battery usage for a variety of UAV missions. The utilization of these models is necessary for the planning of energy-efficient missions and the most effective recharge.

Table 2.3. Different capabilities of UAVs (Manufacturer data).

UAV Model	**Payload (Kg)**	**Max. Flight Time**	**Max. hovering Time (min)**	**Max. Speed (m/s)**	**Max. Flight Distance (Km)**	**Battery Energy (J)**
DJI Mavic 2 Pro	0.91	31 min at consistent 25 kph	29	20	18	213444
DJI Mavic 3	0.89	46 min at consistent 32.4 kph	40	19	30	277200
DJI Air 2	.57	24 min	33	12	18.5	145530
DJI Air 3	.72	46 min at consistent 28.8 kph	42	21	32	225349

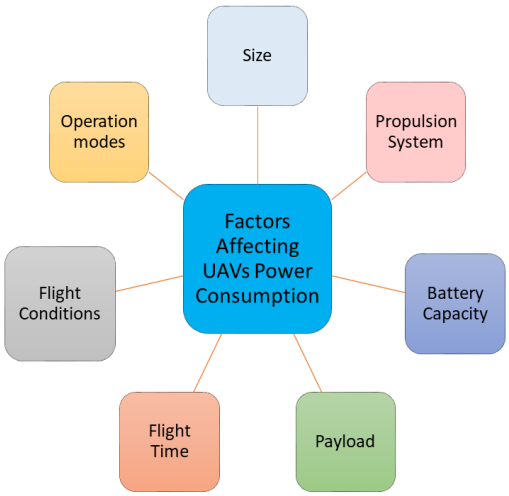

Figure 2.2. Different parameters contributing to the power consumption of the UAV.

To develop comprehensive power consumption models, several parameters that influence energy consumption have been considered. The work in [Zhang et al., 2021] proposed the comprehensive investigation of key parameters contributing to the energy consumption of UAVs used for delivery. Fig. 2.2 shows some important parameters that significantly contribute to the power consumption of UAVs. Various elements that include wind, speed, take-off, landing, hovering, payload, communication, and on-ground power consumption have been investigated in [Abeywickrama et al., 2018b]. The authors in [Góra et al., 2022] provided the universal machine learning model as a substitution for a conventional mathematical model for the power consumption of UAVs. The authors stated that this machine-learning solution is simpler and faster to implement because it does not require prior knowledge of UAV construction. This is a substantial benefit, particularly for multi-UAV system owners who lack the resources to create an analytical power model for each robot. In [Beigi et al., 2022], the state-of-the-art on the UAV power consumption and the general factors that contribute to the power consumption of UAVs during mission

accomplishment are provided. In [Van Huynh et al., 2021], optimal path planning algorithms are proposed for UAVs in order to reduce completion time and overall energy consumption throughout data collecting.

System Model 3

3.1 Overview

This chapter provides the proposed system model, energy model, and UAV trajectory configurations. In the system model, the comprehensive details of path loss model is provided followed with problem formulation. In the energy model, the modes and factors contribution to the energy consumption of UAVs are discussed. In UAV trajectory configurations, UAV movement algorithms are explained.

3.2 Proposed System Model

Disaster scenarios such as a massive earthquake, flood, tsunami, or landslide severely affect people in that area. The majority of structures and infrastructure get damaged, roads are blocked by contamination, and essential commodities such as electricity food and water suffer disruptions. The cellular communication infrastructure has sustained significant damage, specifically, this implies a loss of communication. As a result of disaster, the traditional communication infrastructure can be either completely or partially damaged. Disaster scenarios necessitate the urgent need to establish emergency communication between available devices and responders in that situation. This is crucial to prevent operational interruptions and ensure the timely fulfillment of essential needs for victims, including medicine, water, food, and other necessities.

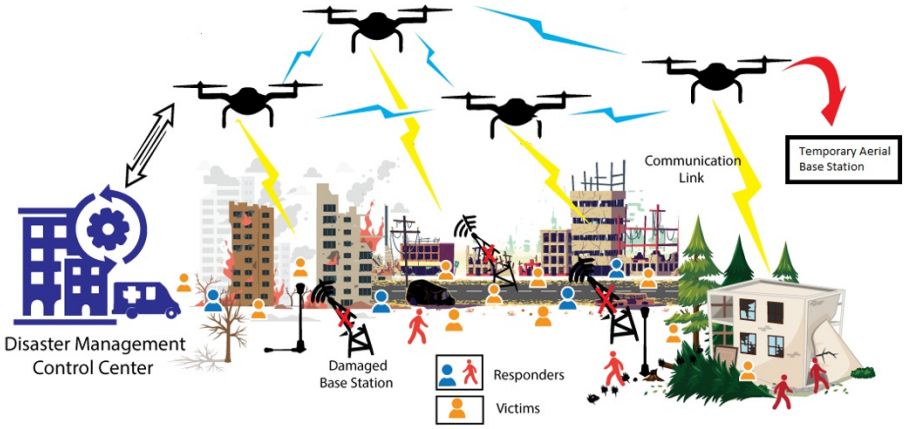

Figure 3.1. System model.

Figure 3.1 shows the system model which illustrates the disaster scenario we are considering for this work. In this scenario, the traditional communication infrastructure is unavailable,

and on-scene devices cannot communicate with the responders. We are considering M devices that are randomly distributed within the disaster zone. The devices can communicate with each other and also connect with a responder through any available UAV in their proximity. Because it is supposed that devices and the UAV are equipped with device-to-device communication interface which enable them to connect with each other. The UAVs are acting as temporary BSs, facilitating communication between responders and on-scene devices. The UAVs enable the line of sight communication link between ground users and temporary BS. However, the link between any ground user to another ground user is non-line of sight. Overall, the goal of this work is to efficiently deploy UAVs to provide full coverage of disaster areas with minimum energy usage for enabling rescue services so that rescue efforts can be done effectively. In the case of our system model, the following assumptions are considered:

- All the ground devices support device-to-device communication technologies such as LTE Direct, WiFi Direct, BLE, etc.
- All the ground devices have the capability of discovering the neighboring devices.
- All the UAVs can directly communicate with the command center.
- Minimum distance between any two UAVs is greater than the coverage radius of the UAV.
- Consider the collision-free environment which implies the height of each UAV greater than obstacles like trees, buildings, etc.
- Any UAV can move to the next waypoint only if it has enough energy to fly back to the starting position.
- Each UAV can carry a payload of up to 500 grams.

3.3 Air-to-Ground (A2G) Path loss

When radio signals radiated from an ABS enter an urban environment, they undergo additional loss in the A2G link due to shadowing and scattering caused by man-made structures. These effects persist even after the signals have traversed free space. The additional loss sustained beyond the path loss in free space is denoted as excessive path loss. This path loss follows a Gaussian distribution. However, for the purposes of this investigation, we focus on its expected mean value rather than its stochastic behavior, thus, η in this context denotes the expected mean value of the excessive path loss. In addition, rapid changes in the propagation environment result in small-scale fluctuations which are not considered. The path loss model we followed is taken from [Al-Hourani et al., 2014b]. The mean A2G path loss can be expressed as:

$$PL_{\xi} = PL_{FS} + \eta_{\xi} \tag{3.3.1}$$

Where the PL_{FS} denotes the free space path loss of signal propagation from ABS to the ground receiver and the unit of PL_{ξ} is decibel (dB). The ξ refers to the propagation class that can be either LOS or non-LOS (NLOS). The NLOS propagation class refers to environment structures causing shadowing and scattering.

To determine the spatial expectation of the path loss, represented as Λ (measured in dB), which occurs between LAP and all ground receivers sharing the same elevation angle θ, the subsequent expectation rule can be expressed as:

$$\Lambda = \sum_{\xi} PL_{\xi} P(\xi, \theta) \tag{3.3.2}$$

where $P(\xi, \theta)$ represents the probability that a certain environmental effect will occur due to its high correlation with the elevation angle. As the $\xi \in (LOS, NLOS)$, the propagation class probabilities are linked as

$$P(NLOS, \theta) = 1 - P(LOS, \theta) \tag{3.3.3}$$

The LOS probability $P(LOS, \theta)$ depends on α, β, and γ statistical parameters. The parameter α refers to the ratio of built-up target area to the total target area. The parameter β refers to the average number of infrastructures or buildings per unit target area. The parameter γ refers to the Rayleigh probability density function that characterizes the distribution of building heights as investigated in [Al-Hourani et al., 2014b]. The LOS probability can be expressed as:

$$P(LOS) = \prod_{n=0}^{m} \left[1 - exp\left(- \frac{[h_{Tx} - \frac{(n+\frac{1}{2})(h_{Tx} - h_{Rx})}{m+1}]}{2\gamma^2} \right) \right] \tag{3.3.4}$$

where m is obtained from $m = (d\sqrt{\alpha\beta} - 1)$ and d represents the distance between the transmitter and the receiver. The h_{Rx} can be disregarded in the case of a low-altitude ABS because it is significantly shorter than both the mean building height and the LAP altitude. Furthermore, the ground distance is calculated as $R = h/tan(\theta)$ ($\theta = arctan(h/R)$), where h represents the altitude of ABS. The α, β, and γ parameters for sub, dense and highrise urban environment are given in Table 3.1 [Al-Hourani et al., 2014a]. Following this trend, the $P(LOS, \theta)$ is approximated to sigmoid function with parameters a and b in [Al-Hourani et al., 2014b] as follow :

$$P(LOS, \theta) = \frac{1}{1 + aexp(-b[\theta - a])} \tag{3.3.5}$$

These parameters are directly linked to the statistical parameters α, β, and γ using surface fitting. The α, β are considered as one variable, and γ is second variable.

$$z = \sum_{j=0}^{3} \sum_{i=0}^{3-j} C_{ij} (\alpha\beta)^i \gamma^j \tag{3.3.6}$$

Where z is the α or β with polynomial coefficient C_{ij} The values of C_{ij} for calculating parameters a and b are used from [Al-Hourani et al., 2014b]. The A2G link is considered

Table 3.1. Parameters for different environments [Al-Hourani et al., 2014a].

Environment	α	β	γ
Sub-Urban	0.1	750	8
Urban	0.3	500	15
Dense-Urban	.5	300	20
Highrise-Urban	.5	300	50

as failed when the total path loss between the ABS and a receiver is greater than the unacceptable level (exceeds the threshold). In the case of ground receivers, this threshold corresponds to a coverage radius of R. This is because all receivers contained within this coverage zone exhibit a path loss equal to or less than PL_{max}. The mathematical expression representing the radius of the coverage zone is as follows:

$$R = d|_{PL_{max}} \tag{3.3.7}$$

Where d is the distance between transmitter and receiver ($d = r$, r is illustrated in Fig. 3.2). To find the optimal altitude of the UAVs, the relation between coverage radius R and UAV altitude is deduced. For that, the Equation 3.3.1 can be written as:

$$PL_{LOS} = 20\log d + 20\log f + 20\log(\frac{4\pi}{c}) + \eta_{LOS} \tag{3.3.8}$$

$$PL_{NLOS} = 20\log d + 20\log f + 20\log(\frac{4\pi}{c}) + \eta_{NLOS} \tag{3.3.9}$$

Where $d = \sqrt{h^2 + R^2}$ ($d = r$, r is illustrated in Fig. 3.2), is the distance between transmitter and receiver at the circular coverage radius of R, and f represents the frequency of the system. The Equation 3.3.2 can be re-expressed as:

$$\Lambda = PL_{NLOS}P(NLOS) + PL_{LOS}P(LOS) \tag{3.3.10}$$

After substitution of equation 3.3.3, 3.3.5, 3.3.7 and 3.3.9 into equation 3.3.10, then after some algebric reduction, the equation 3.3.10 becomes:

$$PL_{max} = \frac{\eta_{LOS} - \eta_{NLOS}}{1 + aexp(-b[arctan(h/R) - a])} + 10\log(h^2 + R^2) + 20\log f + 20\log(\frac{4\pi}{c}) + \eta_{NLOS} \tag{3.3.11}$$

The Equation 3.3.11 is not explicit so the h and R can not be expressed explicitly in terms of each other. To find the optimal altitude h_{opt} that results in maximum coverage, the value of h will be searched that satisfies the critical value of the equation:

$$\frac{\partial R}{\partial h} = 0 \tag{3.3.12}$$

Fig. 3.2 illustrates the impact of different altitude on coverage radius. The optimal altitude h is considered as the upper bound h_{UB} and the average height of the building refers to the lower bound h_{LB}. If we consider the upper bound of h, the resulting coverage radius will be reduced and practically taking the UAV to the altitude of the upper bound is not feasible. Considering the lower bound of h results in more path loss due to NLOS effects and below lower bound can result in collision with buildings. So to avoid such problems, the medium bound h_{MB} is calculated as:

$$h_{MB} = \frac{h_{UB} + h_{LB}}{2} \tag{3.3.13}$$

The circular coverage radius against these bound of h will be obtained from Equation 3.3.7.

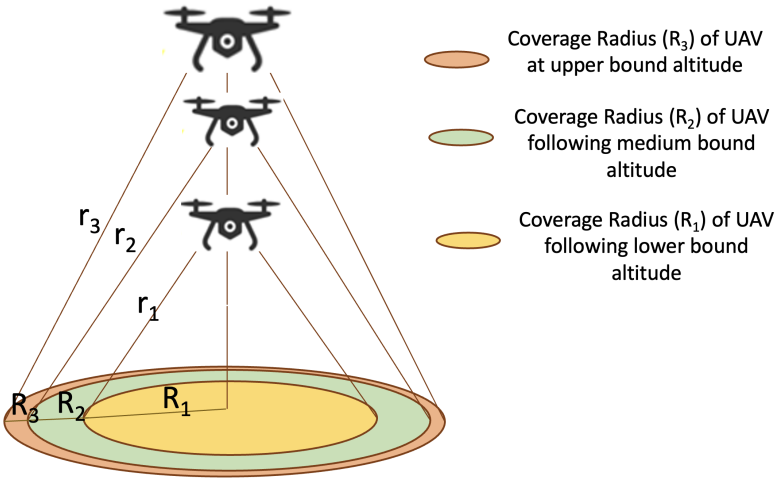

Figure 3.2. Illustration of impact of different altitude on coverage radius.

3.4 Mathematical Method for finding coverage area and non-coverage area

Considering the objective of developing an effective strategy to deploy a minimum number of UAVs to cover the target area completely, We assumed that N UAVs are randomly placed over the target area. The coverage radius of each UAV is R obtained from Equation 3.3.7. As we considered N UAVs over the target area and each with a circular coverage radius R. This implies that each UAV (from the set of N UAVs) covers a portion of the total target area. The percentage that most of the portion of the target area is covered can be defined as:

$$P_{cov} = \frac{\text{Covered Area}}{\text{Total Area}} \tag{3.4.1}$$

As we assumed that each UAV has a circular radius the equation of circle can be used to find the area covered by UAVs. The equation of a circle is expressed as:

$$x^2 + y^2 = R^2 \tag{3.4.2}$$

Where R is equal to the coverage radius of UAV. It can be rewritten as follows:

$$y = \sqrt{R^2 - x^2} \tag{3.4.3}$$

From Equation 3.4.3, area can be obtained as:

$$A = \int_0^x \sqrt{R^2 - x^2}\, dx \tag{3.4.4}$$

Converting Equation 3.4.4 into to polar coordinate system for ease of simplicity. In polar coordinates $x = R\sin\theta$ which implies that $dx = R\cos\theta d\theta$. Using these values in Equation 3.4.4, we get:

$$A = \int_0^\theta \sqrt{R^2 - R^2\sin^2\theta} R\cos\theta\, d\theta \tag{3.4.5}$$

$$A = \int_0^\theta \sqrt{R^2(1 - \sin^2\theta)} R\cos\theta\, d\theta \tag{3.4.6}$$

$$A = \int_0^\theta R^2\cos^2\theta\, d\theta \tag{3.4.7}$$

$$A = R^2 \int_0^\theta \frac{1 + \cos 2\theta}{2}\, d\theta \tag{3.4.8}$$

Where R can be $[0, \infty]$ and θ can be $[0, 2\pi]$. So the area covered by N UAVs can be obtained as:

$$P_{cov} = \frac{\sum_{i=1}^{N} A_i}{\text{Total Area}} \tag{3.4.9}$$

$$P_{cov} = \frac{\sum_{i=1}^{N} R^2 \int_0^{\theta_i} \frac{1+\cos 2\theta}{2}\, d\theta}{\text{Total Area}} \tag{3.4.10}$$

The area under consideration is considered a square grid, the number of waypoints W_{mn} are defined in that square area based on circular radius R so that the complete area will be covered with overlapping circles. Each element in W_{mn} such as $w_{11}, w_{12}, \ldots w_{mn}$ represents the center of small sub-areas of total area. The waypoints in the square area can be expressed in terms of the matrix as follows:

$$W_{mn} = \begin{bmatrix} w_{11} & w_{12} & w_{13} & \ldots & w_{1n} \\ w_{21} & w_{22} & w_{23} & \ldots & w_{2n} \\ \vdots & \vdots & \vdots & \ddots & \vdots \\ w_{m1} & w_{m2} & w_{m3} & \ldots & w_{mn} \end{bmatrix} \tag{3.4.11}$$

Where W_{mn} waypoint matrix with m and n columns, represents the center of mn_{th} circle in the squared area. The value of each entry in the matrix W_{mn} can be 1 or 0. For instance, the value of $w_{11} = 1$ if this waypoint is visited by any UAV otherwise the value of this waypoint will be zero. The probability of total coverage in terms of waypoints can be written as:

$$P_{cov} = \frac{\sum_{i=1}^{m}\sum_{i=1}^{n} W_{mn}}{m \times n} \tag{3.4.12}$$

When each entry in the matrix W_{mn} is 1, then it becomes the matrix of ones and we get the complete coverage that is $P_{cov} = 1$. In this case, cost function is to maximize the P_{cov}. With the help of Equation 3.4.12, we can figure out the uncovered portions of the target area as:

$$P_{non-cov} = 1 - P_{cov} \tag{3.4.13}$$

Equation 3.4.13 gives the percentage of the uncovered portion of the target area.

3.5 Problem Formulation

The coverage problem is formulated as UAV deployment based on linear programming with the aim of minimizing the number of UAVs required to provide coverage over a complete operational area. The following notations are considered to solve the formulated problem:

- A set of waypoints ($W = w_1, w_2, ..., w_m$) is considered over the target area where each point represents the center of circular coverage.
- A set of UAVs ($U = u_1, u_2, ..., u_n$) is considered.
- Each UAV U_i has a specific energy capacity E_{u_i} and coverage radius R_{u_i}.
- If a battery of UAV is depleted and it is unable to continue to the subsequent waypoint, it is required to recharge at the origin point O.

Objective: Ensuring complete area coverage while minimizing the number of UAVs needed to visit all waypoints, considering the limitations imposed by their energy capacities.

Variables: The function f_{ij} is introduced for covering waypoints and it works as follows:

$$f_{ij} = \begin{cases} 1, & \text{if a UAV } u_i \text{ visits the waypoint } w_j \\ 0, & \text{otherwise} \end{cases} \tag{3.5.1}$$

The function Y_i is introduced for minimizing the number of UAVs and it works as follows:

$$Y_i = \begin{cases} 1, & \text{if a UAV } u_i \text{ is used} \\ 0, & \text{otherwise} \end{cases} \tag{3.5.2}$$

Objective Function: Minimize $Z = \sum_{i=1}^{n} Y_i$
Constraints: The constraints which are considered are given by Equation 3.5.3, 3.5.4, and 3.5.5. The constraint in Equation 3.5.3 imposes that each waypoint should be covered by at least one UAV. The constraint in Equation 3.5.4 imposes that the energy of each UAV should be greater than the energy required to cover w_j and return back to the original position O. The constraint in Equation 3.5.5 imposes that UAV is considered as used when it visits at least one waypoint from the given set of waypoints.

$$\sum_{i=1}^{n} f_{ij} \geq 1, \quad \forall w_j \in W \tag{3.5.3}$$

$$E(u_i) \geq \text{ Energy required }, \quad w_j \in W \quad u_i \in U \tag{3.5.4}$$

$$Y_i \geq f_{ij} \quad w_j \in W \quad u_i \in U, \tag{3.5.5}$$

3.6 Energy Model

The UAV Energy model is a critical factor in determining the effectiveness, range, and versatility of configuration schemes of UAVs. It helps to provide insights into energy consumption trends and operating constraints of UAVs. It can lead to better energy management, lowering the operational risks of the UAVs for performing any mission. Efficient energy management results in extended flight duration and ensures a broader operational scope, enhancing the overall utility of UAVs.

The energy model of UAV includes the several critical factors and modes of UAV operations that contribute to the computation of UAV energy [Abeywickrama et al., 2018a]. All the equations of the energy model that are mentioned below, are taken from the work in [Abeywickrama et al., 2018a] and the unit of energy is joule. Authors in [Abeywickrama et al., 2018a] performed the experiment multiple times for UAV energy consumption and recorded the energy consumption over time. Then, they found the expression for average energy consumption for different modes. The details of each mode and the impact of different factors are explained in the following subsections.

3.6.1 Idle Mode

In idle mode, UAVs are turned on and maintained stationary without any rotation of their propellers, maintaining no communication with the base station. In this case, power would be required by the UAV for internal processing, LED indications, and broadcasting a Wi-Fi signal. The energy consumption in the idle mode can be obtained as:

$$E_{Idle} = 8.195 \times t_{Idle} + 0.087 \tag{3.6.1}$$

Where t_{Idle} is the amount of time UAVs stay in idle mode.

3.6.2 Armed Mode

In armed mode, UAVs are turned on and maintained stationary on the ground with the rotation of their propellers, maintaining no communication with the base station. In this case, power would be required by the UAV for propellers in addition to the power required in idle mode. The power consumption in armed mode is greater than in idle mode. The energy consumption in the armed mode can be obtained as:

$$E_{Armed} = 29.027 \times t_{Armed} - 0.087 \tag{3.6.2}$$

Where t_{Armed} is the amount of time UAVs stay in armed mode.

3.6.3 Takeoff Mode

Takeoff mode is the mode where the UAV either ascends to a higher altitude or descends to a lower altitude. The energy consumption due to takeoff can be obtained as:

$$E_{takeoff} = -0.432 \times V^2 + 3.786 * V - 1.224 \tag{3.6.3}$$

Where V is representing the UAV speed during takeoff.

3.6.4 Hovering Mode

The hovering mode is about UAV stationary duration in the air at some fixed position. The UAV continuously consumes energy to remain in its hovering mode. The total energy consumption in hovering mode can be written as:

$$E_{hovering} = (4.917 \times h + 275.204) \times t_{hover} \tag{3.6.4}$$

Where h is the altitude of the UAV during hovering and t_{hover} represents the amount of time the UAV hovers.

3.6.5 Vertical upward Flying Mode

Before the proper flying of the UAVs, they have to take off and fly vertically upward to reach to particular altitude. The power consumption of UAVs while flying vertically upward with a distance of D, can be calculated as:

$$E_{verti} = 315 \times D - 211.261 \tag{3.6.5}$$

3.6.6 Horizontal Flying Mode

Horizontal flying mode refer to the model where UAVs flying in straight line with constant speed. The energy consumption during horizont flying can be expressed as:

$$E_{hori} = 308.709 \times t_{hori} - 0.852 \tag{3.6.6}$$

Where t_{hori} is the amount of time UAVs stay in horizontal flying mode.

3.6.7 Flight Time

The total flight time is the time taken by a single UAV to complete the mission. It is calculated as [Javed et al., 2023]:

$$F_t = \sum_{i=1}^{mn} \frac{dist_i}{V} + T_f + t_{hover} \tag{3.6.7}$$

Where mn is the total waypoints, $dist_i$ is the distance from one waypoint to another waypoint, V is the speed of UAV and T_f is the amount of time UAV fly. The t_{hover} is the hovering time which is considered the same for all UAVs.

3.6.8 Impact of Payload

Payload is the mode in which UAVs are loaded with different amounts of loads and make them hover or fly with their loads. The energy consumption due to the presence of load on UAVs can be given as:

$$E_{payload} = 0.311 \times L + 301.524 \tag{3.6.8}$$

Where L is the amount of load a UAV carries measured in grams.

3.6.9 Impact of GPS

UAVs establish communication with the ground stations for accessing information on travel coordinates using the Global Positioning System (GPS). The energy consumption of UAVs for the time period of t_{GPS} can be obtained as:

$$E_{GPS} = 8.262 \times t_{GPS} \tag{3.6.9}$$

3.6.10 Impact of IR Sensor

An Infrared (IR) sensor mounted on the UAV is responsible for detecting obstacles during UAV movement. IR sensor will be on during the whole UAV operation which results in energy consumption. The energy consumption due to the IR sensor per unit of time t_{IR} is represented as:

$$E_{IR} = 8.262 \times t_{IR} \tag{3.6.10}$$

3.6.11 Impact of Communication

During UAV operation, UAV moves from one point to another to perform its tasks. Before moving to the next point UAV communicates with the command center so that the collision with the other UAVs in the airspace can be avoided which results in energy consumption due to communication. The energy consumption due to communication E_{comm} is as follows.

$$E_{comm} = 8.264 \tag{3.6.11}$$

3.6.12 Total Energy Consumption

The total energy consumption can be expressed as a sum of all energy consumption:

$$\begin{aligned} E_{total} = E_{Idle} + E_{Armed} + E_{takeoff} + E_{hovering} + \\ E_{verti} + E_{hori} + E_{payload} + E_{GPS} + E_{IR} + E_{comm} \end{aligned} \tag{3.6.12}$$

3.7 UAV Movement Cases

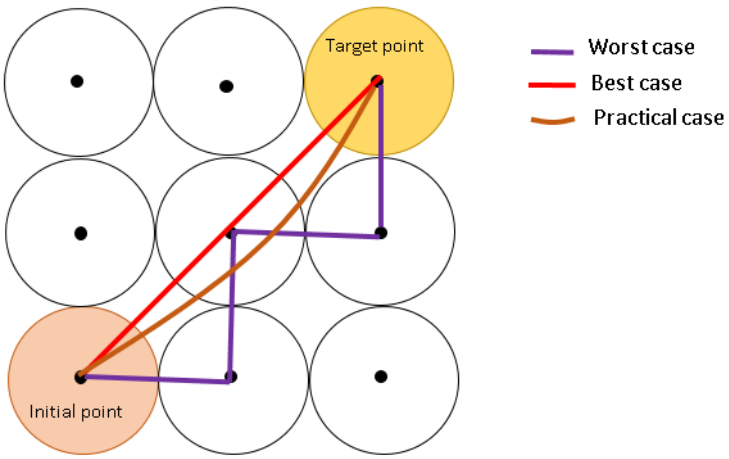

Figure 3.3. UAVs Movement cases.

Fig. 3.3 provides an illustration of UAV movement. There are three cases. The red path shows the best case where UAV moves based on Euclidean distance. In the best case, the UAV moves in a straight line based on the Euclidean distance metric. The purple path shows the worst case where the UAV moves based on Manhattan distance. The equations for calculating Euclidean and Manhattan distance are given in appendix A.4.1 and A.4.2 respectively. In the worst case, the UAV first moves in the x-direction and then in the y-direction to reach the target point. The brown path shows the practical case which is in between the best and worst case. In practical cases, a straight line can not be followed due to the UAVs stability factor.

3.8 UAV Trajectory Configuration

The term configuration refers to the optimal movement planning of UAVs over the target area that maximizes the probability of coverage to gather data from the whole target area while considering certain constraints such as a limited number of UAVs, coverage radius, etc. The section investigates four methodologies for planning UAVs' movement to collect data from a target area. The main objective is to cover the entire area with the minimum number of UAVs. The area under consideration is considered a square grid, with the coverage of UAVs represented by the circular of a predefined radius. First, we approximate the number of UAVs (N) required to cover the whole area. Let the side of the square be S, and the radius of UAV coverage is R_{cov}. The number of UAVs needed to cover the target area without considering overlap can be approximated as $N \approx \frac{S^2}{\sum_{i=1}^{M} \pi R_{cov,i}^2}$. However, in our case, we must ensure complete coverage of the target area. We need more UAVs compared to $N \approx \frac{S^2}{\sum_{i=1}^{M} \pi R_{cov,i}^2}$ due to the circular nature of UAV coverage and the square shape of the area. Additionally, in some cases, we require UAVs at the edges of the square.

It is important to note that all the UAV movement algorithms considered the waypoints in the target area as explained in Equation 3.4.11.

3.8.1 Randomized Coverage Iteration (RCI) algorithm

This algorithm is about random movement planning of the predefined number of UAVs over the target area until all the target area gets covered. In this algorithm, different random paths resulting from the movement of the UAVs are considered while ensuring the combination of all these paths of UAVs gives the probability of coverage equal to 1. Algorithm 1 shows detailed steps illustrating the algorithm that employs a stochastic non-optimal strategy for achieving area coverage. It is initiated by key parameters, including the coverage radius of UAV and the targeted coverage zone. The algorithm randomly traverses the waypoints defined in the area as explained in Equation 3.4.11. A binary matrix is created to reflect areas under surveillance, with binary values indicating the presence or absence of UAVs in the target area. 1 in the binary matrix represents the covered area by any UAV, and 0 represents the area not covered by any UAV. In the next step, the amount of the target area currently covered by the UAVs is calculated. Then, it is evaluated whether the entire target area is covered or not. If the target area is not fully covered, the algorithm updates the configuration to K+1 and moves the UAVs to the next random position. This step updates the paths of UAVs. If all of the waypoints are visited, the process ends, and we have achieved our goal. UAVs cover all the target areas. One flaw in the RCI algorithm is that UAVs may be visited to previously covered positions, potentially leading to redundant coverage and inefficient use of resources. Fig. 3.4 illustrates the resulted path obtained from the RCI algorithm. It can be seen that some waypoints are visited more than once that is highlighted by blue circles.

Algorithm 1 Randomized Coverage Iteration (RCI) algorithm

Require: UAV Coverage Radius, Target Area defined as a Waypoints

1: Start
2: Set Parameters:
- UAV Coverage Radius ▷ Obtained from Eq. 3.3.12
- Obtained matrix of Waypoints (x, y) from Eq. 3.4.11
- Configuration K = 1 ▷ initial configuration index

3: Initially place N UAVs at initial N waypoints
4: **while** Target area is not fully covered **do** :
- UAVs randomly visit the waypoints
- Update Binary Matrix for Coverage
  - Initialize Binary Matrix for coverage
  - For each UAV in Grid:
    - Mark corresponding grid cells as covered within UAV coverage radius
- Calculate the Coverage Area
  - Count the number of ones in the Binary Matrix
- Check if Area is Fully Covered
  - If all cells in the Target area are marked as covered (1), then break the loop
- If not fully covered, increment Configuration K by 1

5: Area Fully Covered
6: **End**

Output: Final path of UAVs that ensure the complete coverage of Target area.

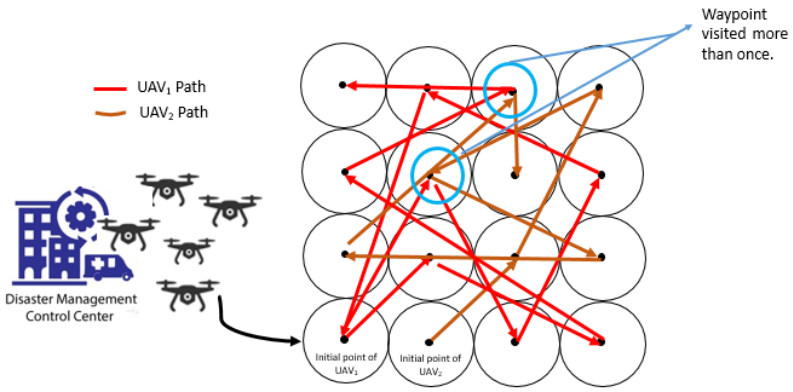

Figure 3.4. Illustration of UAVs path based on Randomized Coverage Iteration (RCI).

3.8.2 Intelligent Randomized Coverage Iteration (IRCI)

The improved version of the UAV movement method is defined as the Intelligent Randomized Coverage Iteration (IRCI). Algorithm 2 shows detailed steps illustrating the algorithm that employs an intelligent random strategy for achieving full area coverage. In the previous approach, UAVs could end up visiting the same waypoints more than once, which was not a good use of resources. In this updated method, once a UAV visits a waypoint, that waypoint is taken off the list for the next time, so this waypoint will not be visited again by any UAV. This ensures that more area gets covered without wasting resources. In this IRCI method, the process starts by deciding how far each UAV can see and making a pattern for where they can go. However, each time when the UAVs visit points, the pattern is updated to remove the existing visited spots of UAVs. This amendment ensures that each UAV visits a new waypoint and unoccupied coordinate, thereby eliminating the possibility of overlapping coverage zones and leading to a more efficient utilization of UAVs. The iterative process continues until all the waypoints are visited. However, with this adjustment, the algorithm advances toward optimal resource deployment by preventing UAVs from reoccupying the exact location across successive iterations. Fig. 3.5 illustrates the resulting path obtained from the IRCI algorithm.

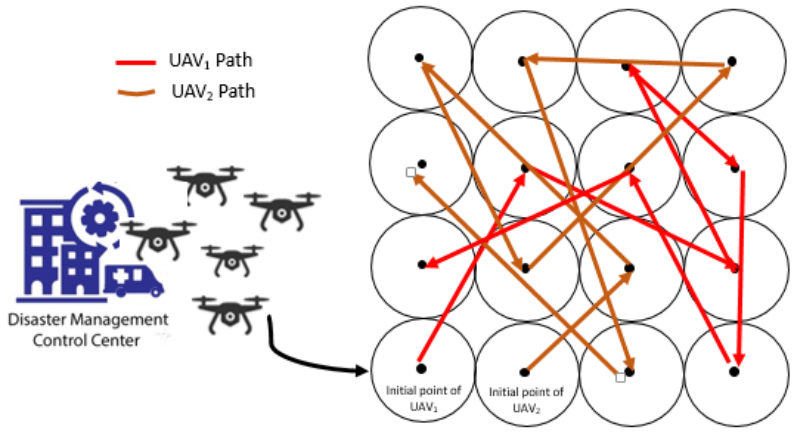

Figure 3.5. Illustration of UAVs path based on Intelligent Randomized Coverage Iteration (IRCI).

In both algorithms, the main objective is to minimize the number of configurations required

Algorithm 2 Intelligent Randomized Coverage Iteration (IRCI) algorithm

Require: UAV Coverage Radius, Target Area defined as a Waypoints

1: Start
2: Set Parameters:
- UAV Coverage Radius ▷ Obtained from Eq. 3.3.12
- Obtained matrix of Waypoints (x, y) from Eq. 3.4.11
- Configuration K = 1 ▷ initial configuration index

3: Initially place N UAVs at initial N waypoints
4: **while** Target area is not fully covered **do**
- UAVs randomly visit the waypoints
- Update Binary Matrix for Coverage
  - Initialize Binary Matrix for coverage
  - For each UAV in Grid:
    - Mark corresponding grid cells as covered within UAV coverage radius
- Calculate the Coverage Area
  - Count the number of ones in the Binary Matrix
- Check if Area is Fully Covered
  - If all cells in the Target area are marked as covered, then break the loop
- If not fully covered, increment Configuration K by 1
- Update the waypoint array by removing the previously visited waypoints

5: Area Fully Covered
6: **End**

Output: Final path of UAVs that ensure complete coverage without visiting the same waypoint more than once.

to achieve complete coverage, which can be mathematically formalized as:

$$P(\text{Area fully covered}|Conf_1, Conf_2, \ldots Conf_n) = 1 \tag{3.8.1}$$

3.8.3 Scan Movement Algorithm

The scan movement algorithm traverses the defined waypoints along the x-direction. Algorithm 3 shows detailed steps illustrating the working of the algorithm for achieving full area coverage. Fig .3.6 shows the illustration of the movement of two UAVs based on scanning along the x-direction. In this scan movement algorithm, N number of UAVs from the disaster management control center are placed on the first $1, 2, 3, \ldots, N$ waypoints on the grid representing the area. Then, N UAVs move to their next waypoints based on the distance of NR so that the collision between N UAVs is avoided. Where R is the coverage radius of the UAV. The waypoints that are visited by N UAVs will not be visited again by any UAV. The UAVs continue to move until all the waypoints are visited. At the end, the order of traversing the waypoints for each UAV is stored as an optimal path. It can be easily seen in Fig.3.6 that two UAVs are placed at the first and second waypoints and they are moving to the next waypoint based on the distance of $2R$.

Algorithm 3 Scan Movement algorithm

Require: Number of UAVs (N), Coverage radius (R), Obtained matrix of Waypoints (x, y) from Eq. 3.4.11

1: Initialize an empty array to store the optimal path for each UAV
   - Place N UAVs to initial N waypoints
   - Initialize an empty list to store the path for the current UAV

2: **while** There are unvisited waypoints **do**
   - Move each UAV to the next waypoint based on the distance of N*R
   - Add the currently visited waypoint to the path list of UAVs
   - Mark the current waypoint as visited
   - Add the path of the current UAV to the list of optimal paths

3: **End**

Output: Optimal path of each UAV that ensures complete coverage.

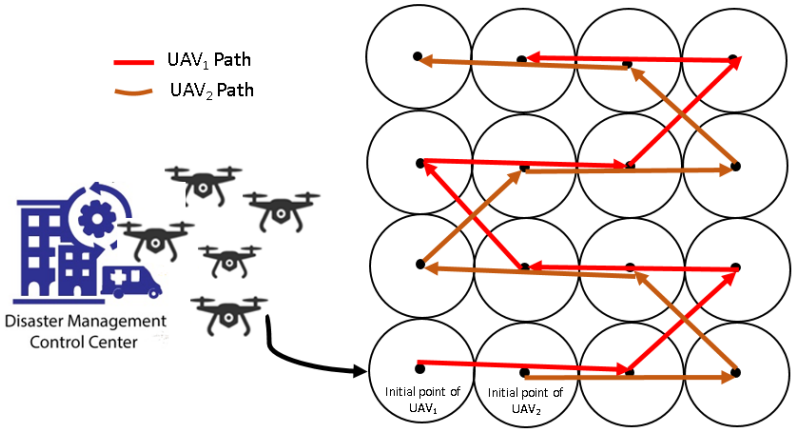

Figure 3.6. UAVs path based on scanning along the x-direction.

3.8.4 Nearest UAV movement Algorithm

This algorithm traverses the defined waypoints in the grid based on minimum Euclidean distance. Algorithm 4 shows detailed steps illustrating the working of the algorithm for achieving full area coverage. Fig .3.7 shows the illustration of the movements of two UAVs based on minimum distance criteria. In this algorithm, the first step is the same as the scan movement algorithm that is N number of UAVs from the disaster management control center are placed on the first $1, 2, 3, \ldots, N$ waypoints on the grid representing the area. Then, each UAV checks the distance from its current position to the first unvisited waypoint in the x-direction and then in the y-direction. The nearest waypoint that has the minimum Euclidean distance from the UAV is selected as the next waypoint. At each UAV movement, the waypoints list is updated by removing the visited waypoints. The waypoints that are visited by N UAVs will be not be visited again by any UAV. The UAVs continue to move based on minimum distance criteria until all the waypoints are visited. At the end, the order of traversing the waypoints for each UAV is stored as an optimal path. It can be easily seen in Fig.3.6 that two UAVs are placed at the first and second waypoints and they are moving to the next waypoint based on the minimum distance. The final path of both UAVs is highlighted with different colors.

Algorithm 4 Nearest UAV Movement algorithm

Require: Number of UAVs (N), Coverage radius (R), Obtained matrix of Waypoints (x, y) from Eq. 3.4.11

1: Initialize an empty array to store the optimal path for each UAV
- Place N UAVs to initial N waypoints
- Initialize an empty list to store the path for the current UAV

2: **while** There are unvisited waypoints **do**
- **For** each UAV in range 1 to N

- Calculate the distance from the current position of UAVs to the unvisited waypoint in the x-direction

- Calculate the distance from the current position of UAVs to the unvisited waypoint in the y-direction

- Compare the distance of the nearest unvisited waypoint in the x-direction and the waypoint in the y-direction

- Select the waypoint with minimum distance as the next waypoint

- Mark the selected waypoint as visited

- Add the currently visited waypoint to the UAV's path list

- Add the path of the current UAV to the list of optimal paths

- **End**

3: **End**

Output: Optimal path of each UAV that ensures complete coverage.

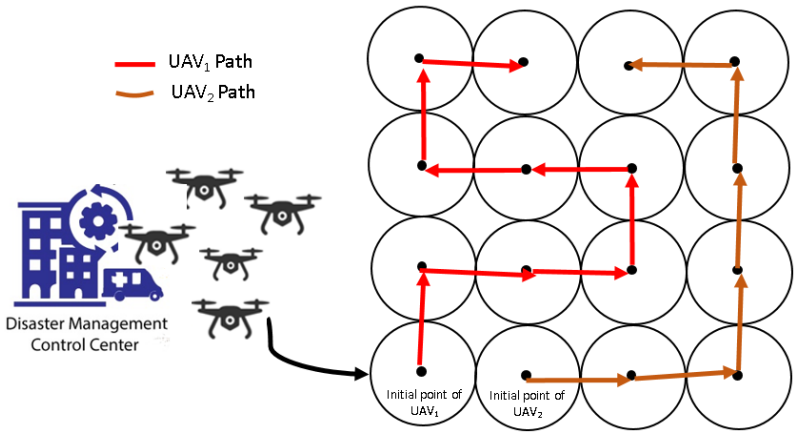

Figure 3.7. UAVs path based on minimum distance

Results and Discussion 4

This chapter provides comprehensive insights into results obtained from simulations. It also presents the comparison between different implemented algorithms.

4.1 Results

All the implementations are done in Python. The values of the parameters used in simulations are provided in Table 4.1. The optimal radius and optimal altitude of UAV for upper and lower bound are calculated using Equation 3.3.7 and 3.3.11, parameters are mentioned in Table 3.1 for different environments. However, the medium bound values are obtained from Equation 3.3.13. Table 4.2, 4.3, and 4.4 provide the obtained values for upper, lower, and medium bound respectively. It is observed that the upper bound has large values of altitude and radius as compared to the lower and medium bounds. The coverage radius of wireless networks can vary significantly depending on the different environments. The suburban environment often has a more extensive coverage radius compared to urban, dense urban, and high-rise urban environments due to fewer construction and obstructions. In urban, high-rise, and dense urban areas, there are more buildings, structures, and other obstacles that can contribute to signal attenuation, reflection, diffraction, and scattering, all of which can result in degradation of the quality of the wireless signal and reduce the effective coverage radius. Stabilizing and maintaining the smooth flight of the UAV at such high altitudes is difficult because higher altitudes require more power for flight. With the limited battery constraints, UAVs are unable to reach and operate efficiently at higher altitudes.

Fig. 4.1 illustrated the full coverage of a target area covered by UAVs. In the figure, the 1000 m x1000 m target area is depicted as densely packed with circles where each circle representing the coverage of a UAV, ensuring that each region of the target area is covered by one of the UAVs.

Table 4.1. Summary of simulation parameters [Abeywickrama et al., 2018b].

Parameters	**Values**
Area (A)	2000m x 2000m= 4,000,000 m^2
Radius (R)	obtained from Table 4.2, 4.3, and 4.4 (Vary for environments)
Speed of UAV (V)	10 m/sec
Idle time t_{Idle}	30 sec
Armed time (t_{Armed})	30 sec
Vertical takeoff speed (V)	3.5 m/sec speed while moving
Hovering time t_{hover}	60 sec to 180 sec
Altitude (h)	Obtained from Equation 3.3.11 PL max equation
Payload L	500 g
Frequency (f)	2GHz=2×10^9Hz
Flight Distance	Flight Speed × Flight Time
Epm	Battery energy (Joules) /flight distance (meters)
Capacity	4000mAh
Voltage	14.8V
Battery energy	Capacity* Voltage * 3.6 = 213120 Joule
Transmitting power	30 dB
Receiving power	-80 dB
Maximum PL	-110 dB
Dimensions (hub-to-hub)	360mm
height	222mm
Weight	865g
Propeller length	222mm
Cost of 1 UAV	15,000 kroner(Assumed)

Table 4.2. Optimal radius and altitude for the upper bound.

Environments	**Optimal radius**	**Optimal altitude**
Sub-Urban	3442.36	1252.92
Urban	2233.11	2010.70
Dense-Urban	1416.26	2022.63
Highrise-Urban	191.66	768.70

Table 4.3. Optimal radius and altitude for the lower bound.

Environments	**Optimal radius**	**Optimal altitude**
Sub-Urban	370.87	8
Urban	402.85	15
Dense-Urban	288.74	20
Highrise-Urban	77.13	50

Table 4.4. Optimal radius and altitude for medium bound.

Environments	**Optimal radius**	**Optimal altitude**
Sub-Urban	2701.22	630.46
Urban	1695.53	1012.85
Dense-Urban	1111.77	1021.32
Highrise-Urban	167.09	409.35

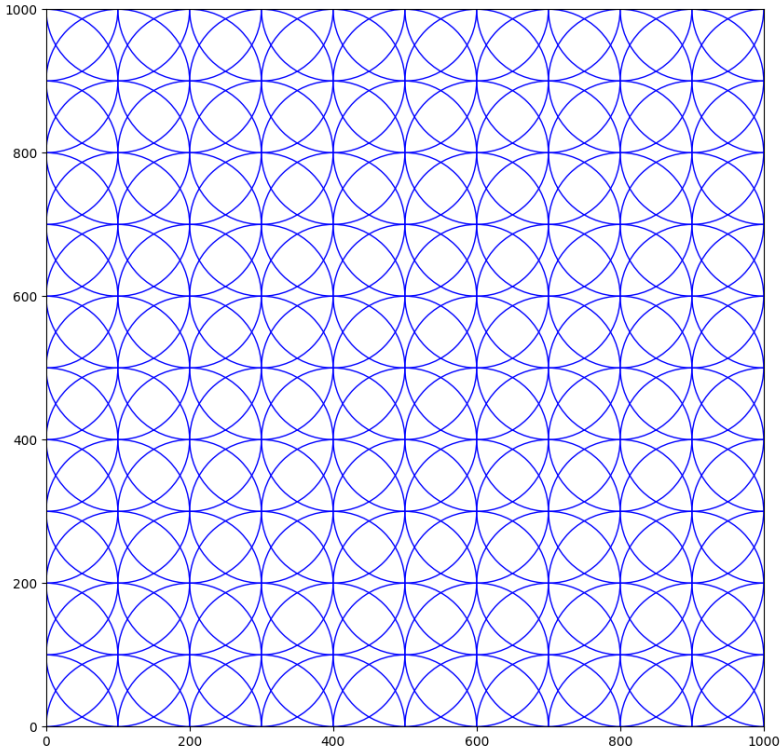

Figure 4.1. UAVs deployment (Overlapping case)

Fig. 4.2 shows the impact of the coverage radius of UAVs on the number of UAVs required to cover the target area of square meters of different dimensions for overlapping case. It can be seen that as the coverage radius of the UAV increases from 100 to 350 meters, the number of UAVs required to cover the target area decreases. However, a further increase in coverage radius has no impact on the number of UAVs. This example is carried out to verify the impact of increasing radii for different area sizes.

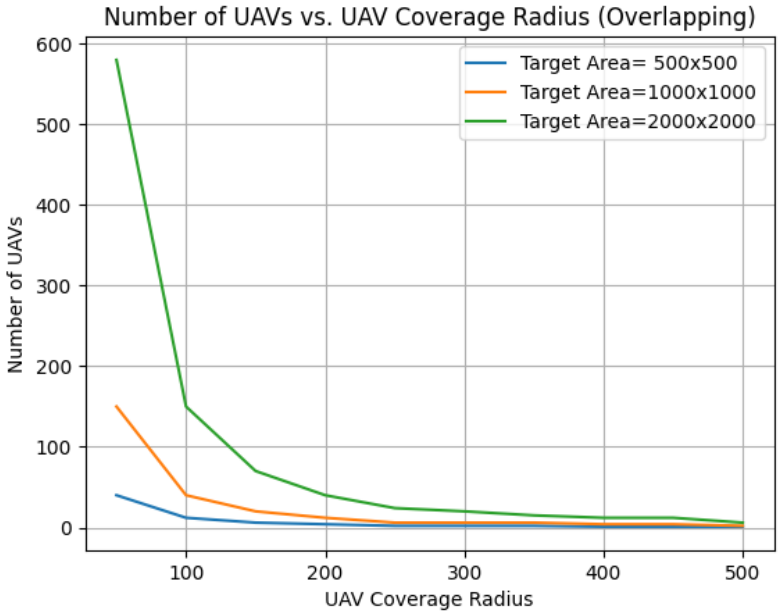

Figure 4.2. Impact of coverage radius on number of UAVs (Overlapping case)

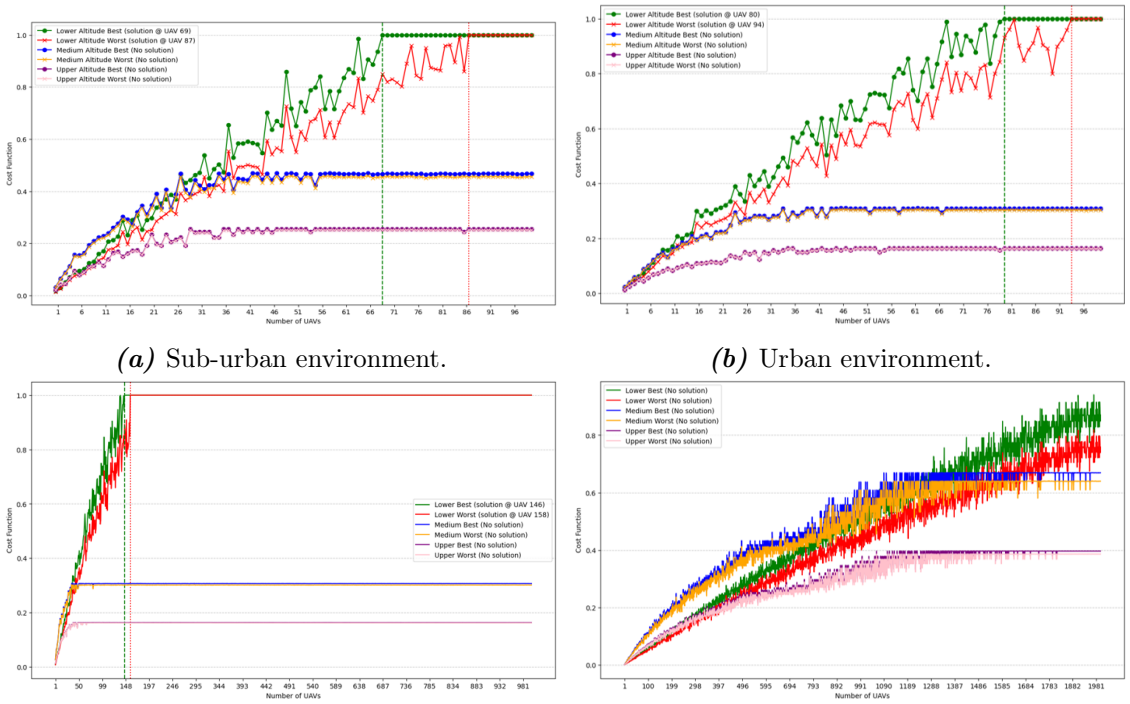

(a) Sub-urban environment.

(b) Urban environment.

(c) Dense-urban environment.

(d) Highrise-urban environment

Figure 4.3. Performance analysis of RCI algorithm in different environment considerations in terms coverage cost vs Number of UAVs.

The performance analysis of each developed algorithm is evaluated for the lower, medium, and upper bound altitude in four different environments in terms of a cost function defined as P_{cov} in Equation 3.3.13. The value of altitudes for upper, lower, and medium bound for each environment is taken from Table 4.2, 4.3, and 4.4, respectively.
The cost function shows the percentage of coverage area. Coverage area is calculated as the

Battery energy of a UAV/ required energy to cover the target area. Battery energy for a UAV is mentioned in Table 4.1. The required energy for each UAV to cover the target area for different environments of all algorithms can be seen in Fig. A.2, Fig. A.6, Fig. A.10 and Fig. A.14. The cost function value equal to 0 refers to the 0 percent area coverage and 1 refers to the 100 percent area coverage. When the target area is covered completely, this way, we obtain the exact number of UAVs needed to cover 100 percent area in different environments. The worst and the best cases that are considered are explained in Section 3.7.

Fig. 4.3 shows the performance analysis of the RCI algorithm in different environment considerations. In Fig. 4.3 (a), the cost function is analyzed with respect to the number of UAVs in a suburban environment. It can be seen that the lower bound altitude with the best case gets the maximum cost value of 1 at 69 number of UAVs and the lower bound altitude with the worst case gets the maximum cost value of 1 at 87 number of UAVs. That means the lower altitude with best and worst case provides the 100 percent coverage of the target area with 69 and 87 number of UAVs respectively. However, the medium and upper-bound cases provide no solution. These cases have the maximum cost value of 0.45 and 0.25 respectively which implies that these cases provide the 45 and 25 percent coverage of the target area. In Fig. 4.3 (b) the cost function is analyzed with respect to the number of UAVs in the urban environment. It can be seen that the lower bound altitude with the best case gets the maximum cost value of 1 at 80 number of UAVs and the lower bound altitude with the worst case gets the maximum cost value of 1 at 94 number of UAVs. That means the lower altitude with best and worst case provides the 100 percent coverage of the target area with 80 and 94 number of UAVs respectively. However, the medium and upper-bound cases provide no solution. These cases have the maximum cost value of 0.25 and 0.18 respectively which implies that these cases provide the 25 and 18 percent coverage of the target area. In Fig. 4.3 (c) the cost function is analyzed with respect to the number of UAVs in a sub-urban environment. It can be seen that the lower bound altitude with the best case gets the maximum cost value of 1 at 148 number of UAVs and the lower bound altitude with the worst case gets the maximum cost value of 1 at 157 number of UAVs. That means the lower altitude with best and worst case provides the 100 percent coverage of the target area with 148 and 157 number of UAVs respectively. However, the medium and upper bound cases provide no solution as they do not satisfy the constraint in Equation 3.5.4. These cases have the maximum cost value of 0.25 and 0.16 respectively which implies that these cases provide the 25 and 16 percent coverage of the target area. In Fig. 4.3 (d) the cost function is analyzed with respect to the number of UAVs in a sub-urban environment. It can be seen that all the cases provide no solution.

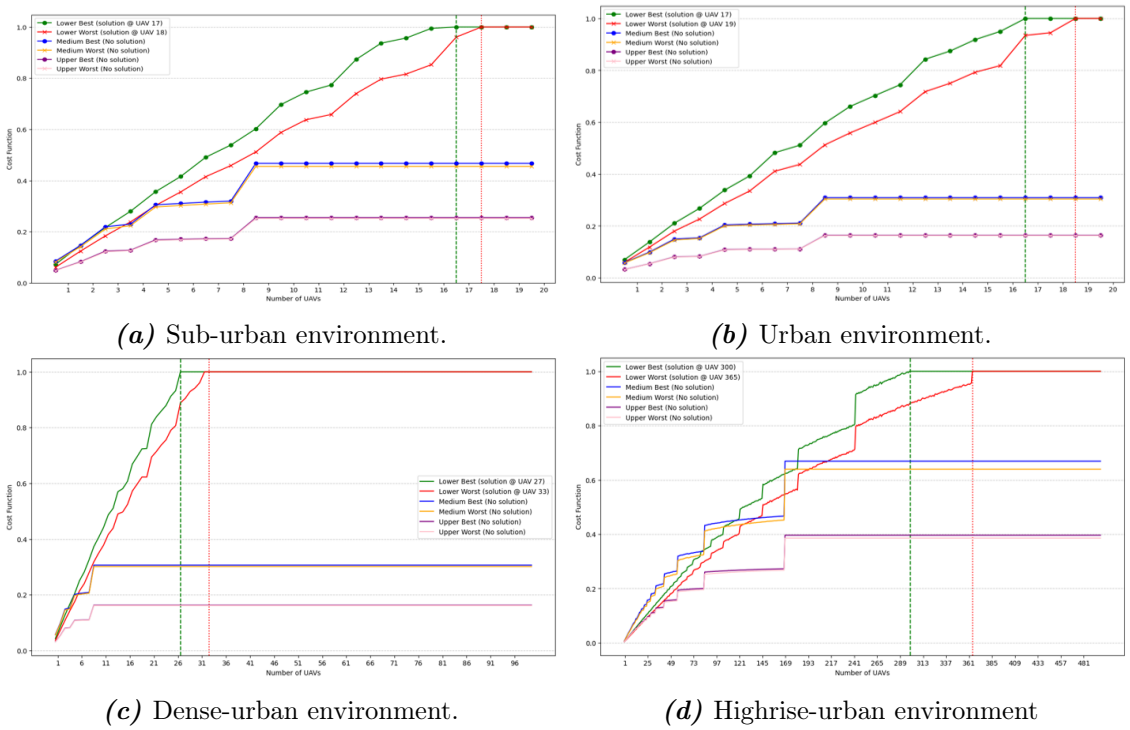

(a) Sub-urban environment. ***(b)*** Urban environment.

(c) Dense-urban environment. ***(d)*** Highrise-urban environment

Figure 4.4. Performance analysis of optimal IRCI algorithm in different environment considerations in terms coverage cost vs Number of UAVs.

Fig. 4.4 shows the performance analysis of the non-optimal RCI algorithm in different environment considerations. In Fig. 4.4 (a), the cost function is analyzed with respect to the number of UAVs in a sub-urban environment. It can be seen that the lower bound altitude with the best case gets the maximum cost value of 1 at 17 number of UAVs and the lower bound altitude with the worst case gets the maximum cost value of 1 at 18 number of UAVs. That means the lower altitude with best and worst case provides the 100 percent coverage of the target area with 17 and 18 number of UAVs respectively. However, the medium and upper bound cases provide no solution. These cases have the maximum cost value of 0.46 and 0.23 respectively which implies that these cases provide the 46 and 23 percent coverage of the target area. In Fig. 4.4 (b) the cost function is analyzed with respect to the number of UAVs in an urban environment. It can be seen that the lower bound altitude with the best case gets the maximum cost value of 1 at 17 number of UAVs and the lower bound altitude with the worst case gets the maximum cost value of 1 at 19 number of UAVs. That means the lower altitude with best and worst case provides the 100 percent coverage of the target area with 17 and 19 number of UAVs respectively. However, the medium and upper bound cases provide no solution. These cases have the maximum cost value of 0.27 and 0.18 respectively which implies that these cases provide the 27 and 18 percent coverage of the target area. In Fig. 4.4 (c) the cost function is analyzed with respect to the number of UAVs in a sub-urban environment. It can be seen that the lower bound altitude with the best case gets the maximum cost value of 1 at 27 number of UAVs and the lower bound altitude with the worst case gets the maximum cost value of 1 at 33 number of UAVs. That means the lower altitude with best and worst case provides the 100 percent coverage of the target area with 27 and 33 number of UAVs respectively. However, the medium and upper bound cases provide no solution. These cases have the maximum

cost value of 0.25 and 0.17 respectively which implies that these cases provide the 25 and 17 percent coverage of the target area. In Fig. 4.3 (d) the cost function is analyzed with respect to the number of UAVs in a sub-urban environment. It can be seen that all the lower bound altitudes with best case get the maximum cost value of 1 at 300 number of UAVs and lower bound altitudes with worst case get the maximum cost value of 1 at 365 number of UAVs. That means the lower altitude with best and worst case provides the 100 percent coverage of the target area with 300 and 365 number of UAVs respectively. However, the medium and upper bound cases provide no solution. As these cases have got the maximum cost value of 0.64 and 0.4 respectively which implies that these cases provide the 64 and 40 percent coverage of the target area.

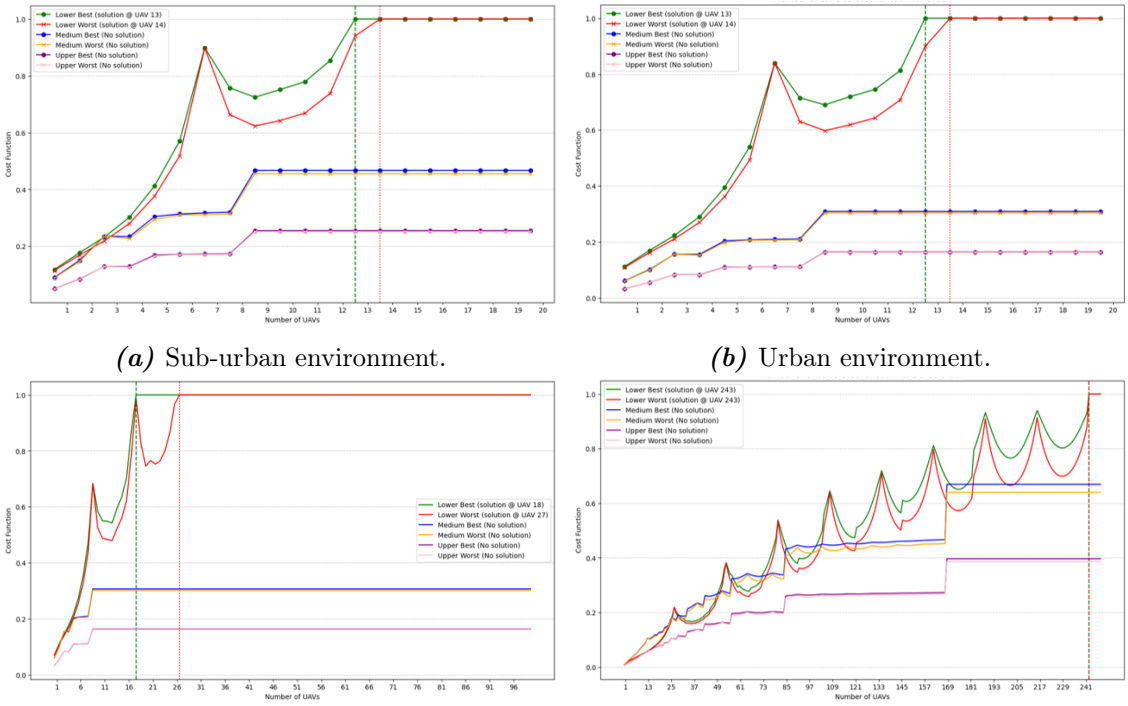

(a) Sub-urban environment.

(b) Urban environment.

(c) Dense-urban environment.

(d) Highrise-urban environment

Figure 4.5. Performance analysis of scan movement algorithm in different environment considerations in terms coverage cost vs Number of UAVs.

Fig. 4.5 shows the performance analysis of the scan movement algorithm in different environment considerations. In Fig. 4.5 (a), the cost function is analyzed with respect to the number of UAVs in a sub-urban environment. It can be seen that the lower bound altitude with the best case gets the maximum cost value of 1 at 13 number of UAVs and the lower bound altitude with the worst case gets the maximum cost value of 1 at 14 number of UAVs. That means the lower altitude with best and worst case provides the 100 percent coverage of the target area with 13 and 14 number of UAVs respectively. However, the medium and upper bound cases provide no solution. These cases have the maximum cost value of 0.43 and 0.23 respectively which implies that these cases provide the 43 and 23 percent coverage of the target area. In Fig. 4.5 (b) the cost function is analyzed with respect to the number of UAVs in an urban environment. It can be seen that the lower bound altitude with the best case gets the maximum cost value of 1 at 13 number of UAVs and the lower bound altitude with the worst case gets the maximum cost value of 1 at 14

number of UAVs. That means the lower altitude with best and worst case provides the 100 percent coverage of the target area with 13 and 14 number of UAVs respectively. However, the medium and upper bound cases provide no solution. These cases have the maximum cost value of 0.25 and 0.19 respectively which implies that these cases provide the 25 and 19 percent coverage of the target area. In Fig. 4.5 (c) the cost function is analyzed with respect to the number of UAVs in a sub-urban environment. It can be seen that the lower bound altitude with the best case gets the maximum cost value of 1 at 18 number of UAVs and the lower bound altitude with the worst case gets the maximum cost value of 1 at 27 number of UAVs. That means the lower altitude with best and worst case provides the 100 percent coverage of the target area with 18 and 27 number of UAVs respectively. However, the medium and upper bound cases provide no solution. These cases have the maximum cost value of 0.25 and 0.18 respectively which implies that these cases provide the 25 and 18 percent coverage of the target area. In Fig. 4.5 (d) the cost function is analyzed with respect to the number of UAVs in a sub-urban environment. It can be seen that all the lower bound altitudes with best case get the maximum cost value of 1 at 243 number of UAVs and lower bound altitudes with worst case get the maximum cost value of 1 at 243 number of UAVs. That means the lower altitude with best and worst case provides the 100 percent coverage of the target area with 243 and 243 number of UAVs respectively. However, the medium and upper bound cases provide no solution. These cases have the maximum cost value of 0.62 and 0.4 respectively which implies that these cases provide the 62 and 40 percent coverage of the target area.

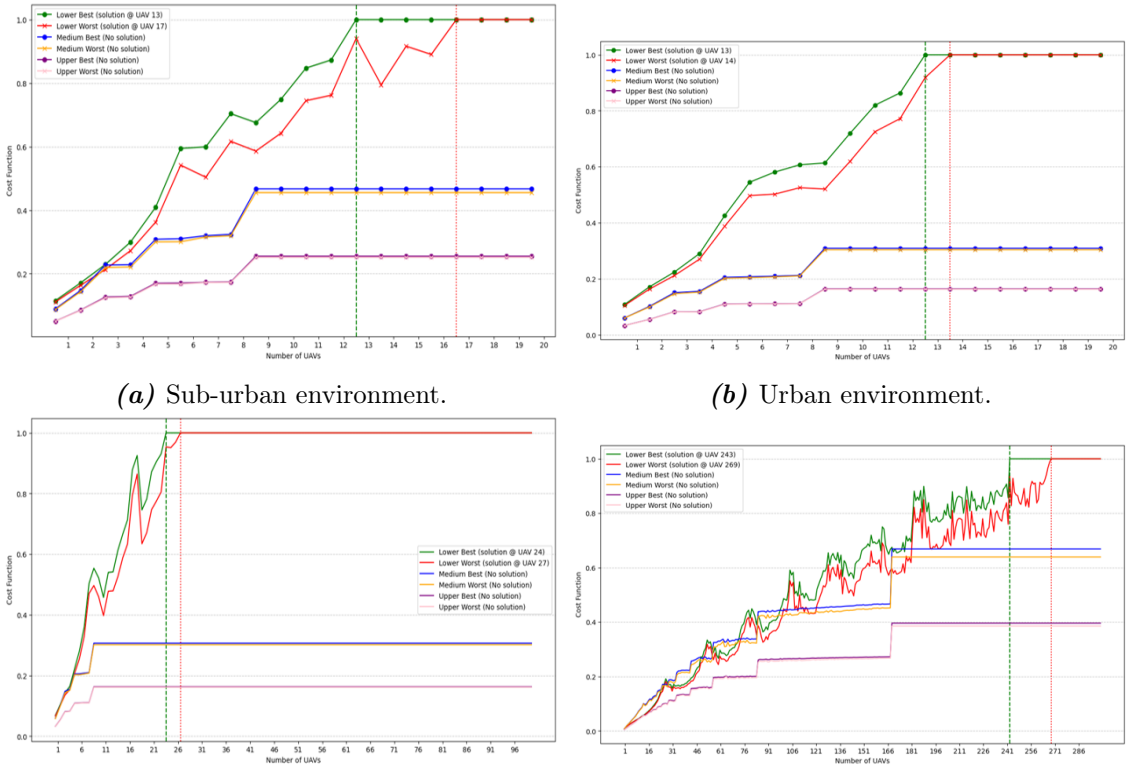

(a) Sub-urban environment.

(b) Urban environment.

(c) Dense-urban environment.

(d) Highrise-urban environment

Figure 4.6. Performance analysis of nearest movement algorithm in different environment considerations in terms coverage cost vs Number of UAVs.

Fig. 4.6 shows the performance analysis of the non-nearest movement algorithm in different environment considerations. In Fig. 4.6 (a), the cost function is analyzed with respect to the number of UAVs in a sub-urban environment. It can be seen that the lower bound altitude with the best case gets the maximum cost value of 1 at 13 number of UAVs and the lower bound altitude with the worst case gets the maximum cost value of 1 at 17 number of UAVs. That means the lower altitude with best and worst case provides the 100 percent coverage of the target area with 13 and 17 number of UAVs respectively. However, the medium and upper bound cases provide no solution. These cases have the maximum cost value of 0.43 and 0.23 respectively which implies that these cases provide the 43 and 23 percent coverage of the target area. In Fig. 4.5 (b) the cost function is analyzed with respect to the number of UAVs in an urban environment. It can be seen that the lower bound altitude with the best case gets the maximum cost value of 1 at 13 number of UAVs and the lower bound altitude with the worst case gets the maximum cost value of 1 at 14 number of UAVs. That means the lower altitude with best and worst case provides the 100 percent coverage of the target area with 13 and 14 number of UAVs respectively. However, the medium and upper bound cases provide no solution. These cases have the maximum cost value of 0.25 and 0.19 respectively which implies that these cases provide the 25 and 19 percent coverage of target area. In Fig. 4.5 (c) the cost function is analyzed with respect to the number of UAVs in a sub-urban environment. It can be seen that the lower bound altitude with the best case gets the maximum cost value of 1 at 24 number of UAVs and the lower bound altitude with the worst case gets the maximum cost value of 1 at 27 number of UAVs. That means the lower altitude with best and worst case provides the 100 percent coverage of the target area with 24 and 27 number of UAVs respectively. However, the medium and upper-bound cases provide no solution. These cases have the maximum cost value of 0.25 and 0.18 respectively which implies that these cases provide the 25 and 18 percent coverage of the target area. In Fig. 4.5 (d) the cost function is analyzed with respect to the number of UAVs in a sub-urban environment. It can be seen that all the lower bound altitudes with best case get the maximum cost value of 1 at 243 number of UAVs and lower bound altitudes with worst case get the maximum cost value of 1 at 269 number of UAVs. That means the lower altitude with best and worst case provides the 100 percent coverage of target area with 243 and 269 number of UAVs respectively. However, the medium and upper bound cases provide no solution. These cases have the maximum cost value of 0.62 and 0.4 respectively which implies that these cases provide the 62 and 40 percent coverage of the target area.

Table 4.5 provides the comparison of algorithms for lower bound of different environments. In Fig. 4.3 to 4.6, it is noted that all the algorithms provided the 100 percent coverage in lower bound. Therefore, in this Table 4.5, the number of UAVs required to provide complete coverage are compared for four different environment cases. It can be seen that scan movement algorithm required minimum number of UAVs for complete coverage in all cases. Table 4.6 provide the comparison of algorithms in terms of budget cost. The budget cost for each algorithm cases is calculated using the cost of 1 UAV $\times$ Number of UAVs required where the cost of 1 UAV given in Table 4.1. It can be seen that the scan algorithm have the minimum cost for environment cases as compared to other algorithms because it requires minimum number of UAVs compared to other.

From Fig. 4.3 to 4.6 and above tables, it is observed that in all the cases, the sub-urban

Table 4.5. Algorithms comparison

Environment	**Bound**	**RCI Algorithm**	**IRCI Algorithm**	**Scan Movement Algorithm**	**Nearest Movement Algorithm**
Sub-Urban	Lower best	69 UAVs	17 UAVs	13 UAVs	13 UAVs
	Lower worst	87 UAVs	18 UAVs	14 UAVs	17 UAVs
Urban	Lower best	80 UAVs	17 UAVs	13 UAVs	13 UAVs
	Lower worst	94 UAVs	19 UAVs	14 UAVs	14 UAVs
Dense-Urban	Lower best	146 UAVs	27 UAVs	18 UAVs	24 UAVs
	Lower worst	158 UAVs	33 UAVs	27 UAVs	27 UAVs
Highrise-Urban	Lower best	No solution	300 UAVs	243 UAVs	243 UAVs
	Lower worst	No solution	365 UAVs	243 UAVs	269 UAVs

Table 4.6. Algorithms comparison in terms of budget cost.

Environment	**Bound**	**RCI Algorithm**	**IRCI Algorithm**	**Scan Movement Algorithm**	**Nearest Movement Algorithm**
Sub-Urban	Lower best	1035K	255K	195K	195K
	Lower worst	1305K	270K	210K	255K
Urban	Lower best	1200K	255K	195K	195K
	Lower worst	1410K	285K	210K	210K
Dense-Urban	Lower best	2190K	405K	270K	360K
	Lower worst	2370K	495K	405K	405K
Highrise-Urban	Lower best	No solution	4500K	3645K	3645K
	Lower worst	No solution	5475K	3645K	4035K

environment with lower bound we get the 100 percent coverage with the minimum number of UAVs compared to other environments. Also, the scan algorithm had the minimum cost for all environment cases. It is noted that at medium and upper altitude cases, the complete coverage solution did not exist. At these higher altitudes, although the UAVs have a broader coverage radius, but certain limitation arises due to the battery power constraints inherent to UAV technology. Due to these limitations, UAVs are unable to reach and operate efficiently. In addition, it is noted that the scan movement algorithms are outperforming other algorithms with the minimum number of UAVs. The nearest movement algorithm is performing better than RCI and IRCI. The scan and nearest movement algorithm provides a better coverage percentage than other algorithms for medium and higher bound cases in all environments. It is also noted that the RCI algorithm has no solution for all bound cases in highrise-urban environments. Other algorithms provide the solution for lower bound cases in highrise-urban environments for a significantly higher number of UAVs.

The performance of the algorithms in terms of total distance traveled, energy consumption, number of configurations and total flight time for lower, medium, and upper bound altitude in four different environments, is evaluated in the appendix from Fig. A.1 to A.16.

4.2 Findings

This section provides the findings obtained from results analysis and discussion. The four different UAV movement algorithms including RCI, IRCI, Scan, and nearest, are developed to provide the complete coverage of target area. These algorithms were evaluated for four different environments, sub-urban, urban, dense-urban, and highrise-urban. Three bounds lower, upper, and medium are defined for UAV altitude. From results it is found that

- All the algorithms provided the 100 percent coverage for lower bound in sub-urban environment. The coverage radius of wireless networks significantly vary depending on different environments. The sub-urban environment often experiences the extensive coverage compared to other environments due to fewer obstructions and less constructions that allow for more straightforward propagation models where signals can travel farther without significant loss. However, in case of urban, high-rise, and dense urban areas, there are more buildings, structures, and other obstacles that causes signal attenuation, reflection, diffraction, and scattering, and affect the quality of the wireless connection resulting in reduced the effective coverage area.
- Among all the algorithms, scan algorithm provided the complete coverage with minimum number of UAVs for lower bound in all environments. It is noted that at medium and upper altitude cases, the complete coverage solution did not exist. Altitudes at medium and upper bound were higher, at higher altitudes although UAV have large coverage radius but UAV requires more power for sustained flight. Due to certain critical limitation such as UAV battery power constraints, UAVs are unable to reach and operate efficiently at these heights. Consequently, despite the potential for greater ground coverage, no viable solution was found for UAV operations at medium and upper altitudes under our current UAV battery constraints.
- As scan algorithm requires minimum number of UAVs for complete coverage for all environment cases which results in minimum budget cost. But less number of UAVs

lead to increased rescue time for completing rescue operation as the rescue time depends on flight time which can be seen in Fig. A.12 that less number of UAVs require more flight time. In the cases of other environments, the number of UAVs required for complete coverage increased which means budget cost also increases. But with the increased number of UAVs, response time for rescue operation decreases because more UAVs are involved to complete the operation as shown in Fig. A.4, A.8, and A.16.

- It is also observed that in all the environments the energy consumption decreases with the increased number of UAVs as shown in A.2, A.6, A.10 and A.14. Because when the number of UAVs increases the flight time to cover the whole area decreases which results in decreased energy consumption.
- Given the limited UAV resources, the scan algorithm will be performed because it require minimum number of UAVs as compared to other algorithms at the cost of increased response time.

Conclusion 5

This work focused on the deployment of UAVs as aerial base stations for providing complete coverage in disaster scenarios to enable rescue operations and services to the victims using the minimum available resources as detailed by the problem statement:
How to implement quick and robust communication service with efficient resource management to effectively perform and manage rescue operations?
In this context, four different UAV movement algorithms: Randomized Coverage Iteration (RCI), Intelligent Randomized Coverage Iteration (IRCI), scan movement, and nearest movement, were developed to provide complete coverage with the optimal number of UAVs and minimum energy consumption. The performance of these algorithms was evaluated for the three different bounds of altitudes: lower, medium, and upper bound altitude in four different environments. The four different environments: suburban, urban, dense-urban, and highrise-urban were considered. The performance was analyzed in terms of coverage, average total distance travelled, average energy consumption, and number of configurations. It was noted that all the algorithms provide complete coverage in suburban environments with lower altitude bounds. The medium and upper altitude cases did not provide the complete coverage solution. Because at higher altitudes UAVs are unable to reach and operate efficiently due to their battery constraints. It is observed that the scan algorithm in the sub-urban environment with a lower altitude bound outperforms in terms of the minimum number of UAVs as compared to other algorithms. It is also observed that in all the environments the average distance travel, energy consumption, and flight time decrease with the increased number of UAVs because when the number of UAVs increases the average distance and flight time of a single to cover the whole area decreases which results in decreased energy consumption. Given the limited UAV resources, the scan algorithm will be performed because it requires a minimum number of UAVs as compared to other algorithms at the cost of increased response time. It is important to note that these results may change for other UAVs with different simulation parameters. It can be concluded that lower altitude settings offer superior performance for the considered simulation parameters. In future, our aim is to test the developed algorithm in real-time to ensure their practical efficacy. In addition, we will incorporate the Intelligent Reflective Surface (IRS) technology to further UAV coverage capabilities and response time. The limitation of this work is that this solution can not be useful in dense and highly dense urban environments because in these environments, UAVs need to operate at high altitudes and at high altitudes our solution is not performing good. In future, We will work on customized UAVs specifically their batteries designed for high and medium-altitude operations.

Appendix

Appendix A

This appendix shows the performance of the algorithms in terms of total distance traveled, energy consumption, number of configurations and total flight time for lower, medium, and upper bound altitude in four different environments. These metrics show the average total distance traveled, number of configurations, and total flight time of a single UAV.

A.1 RCI Algorithm

Fig. A.1 shows the average total distance traveled by a single UAV of RCI algorithm for lower, medium, and upper bound altitude in four different environments. The average total distance traveled is calculated by $\sum_{i=1}^{mn} dist_i$, where mn is the total waypoints and $dist_i$ is the distance between one waypoint to another waypoint. It can be seen that as the number of UAVs increases, the average distance traveled by a single UAV decreased. For all the environments, the average distance traveled by a single UAV for lower bound altitude is greater than other bound cases. Because in lower bound less number of UAVs are required to provide full coverage as compared to other bounds cases.

Fig. A.2 shows the average energy consumption of RCI algorithm for lower, medium, and upper bound altitude in four different environments. The average energy consumption is calculated using Equation 3.6.12. It can be seen that in all the environments the energy consumption decreases with the increased number of UAVs because when the number of UAVs increases the flight time to cover the whole area decreases which results in decreased energy consumption. In Fig. A.2 (a), the medium bound cases have lower energy consumption compared to other bound cases. However, in other environments (b), (c), and (d), all the bound cases have no significant difference between energy consumption. This is due to the random movements of UAVs.

Fig. A.3 shows the average number of configurations of a single UAV of RCI algorithm for different bound cases in all environments. The term configuration refer to the movement of UAV from one point to another. It can be seen that the average number of configurations of single UAV decreases with increase in the number of UAVs. Because when the number of UAVs increases, the total configurations are divided between the UAVs, so the average number of configuration for single UAV decreases.

Fig. A.4 shows the average flight of a single UAV of RCI algorithm for different bound cases in all environments. The average flight time ic calculated using Equation 3.6.7. It can be seen that as the number of UAVs increases, the average flight time of a single UAV decreased. For all the environments, the average distance traveled by a single UAV for lower bound altitude is greater than other bound cases. Because in lower bound less

number of UAVs are required to provide full coverage as compared to other bounds cases.

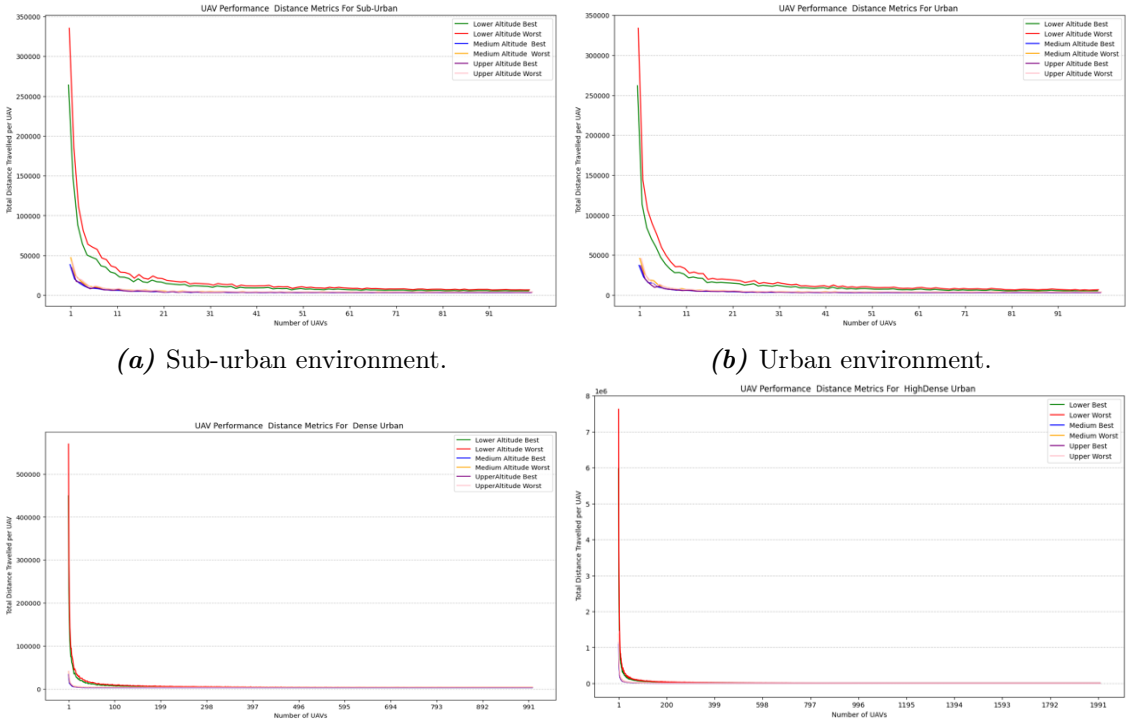

(a) Sub-urban environment.

(b) Urban environment.

(c) Dense-urban environment.

(d) Highrise-urban environment

Figure A.1. Performance analysis of RCI algorithm in different environment considerations in terms of total distance traveled by UAVs to cover the target area.

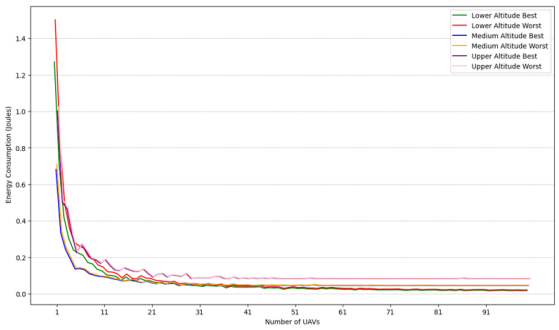

(a) Sub-urban environment. The scale of the y-axis for energy consumption is 10^7

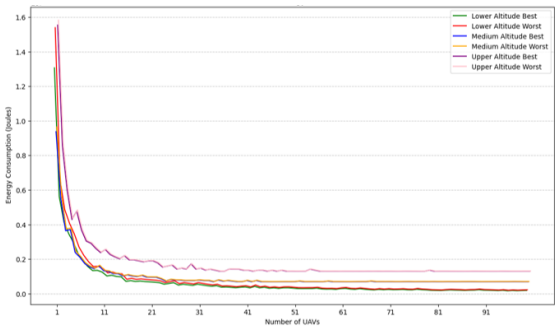

(b) Urban environment. The scale of the y-axis for energy consumption is 10^7

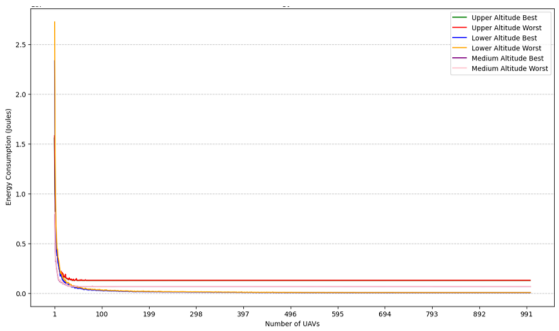

(c) Dense-urban environment. The scale of the y-axis for energy consumption is 10^7

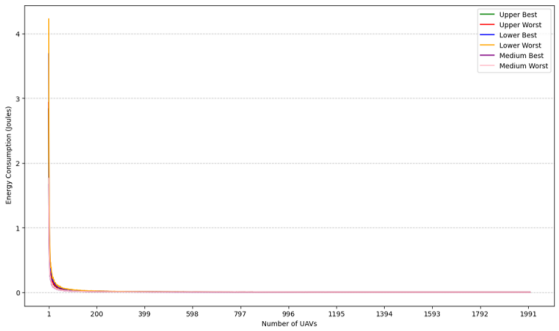

(d) Highrise-urban environment. The scale of the y-axis for energy consumption is 10^7

Figure A.2. Performance analysis of RCI algorithm in different environment considerations in terms of energy consumption by UAVs to cover the target area.

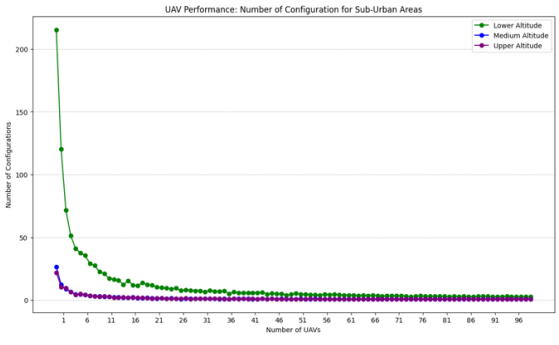

(a) Sub-urban environment.

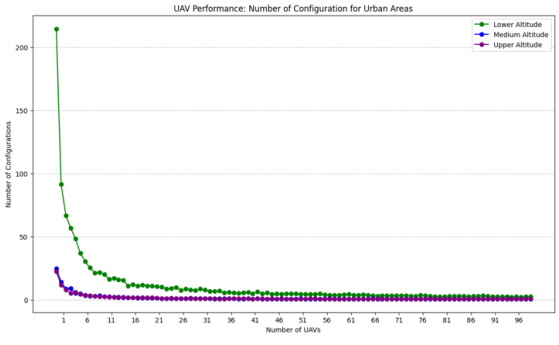

(b) Urban environment.

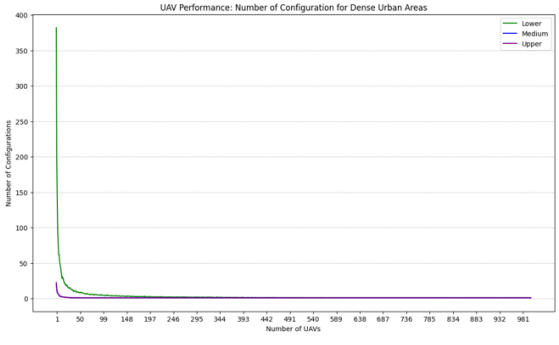

(c) Dense-urban environment.

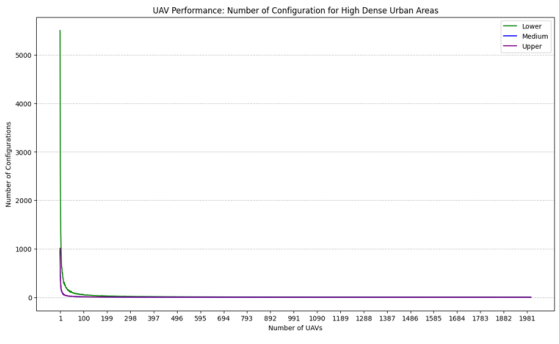

(d) Highrise-urban environment

Figure A.3. Performance analysis of RCI algorithm in different environments in terms of number of configurations required to cover the target area.

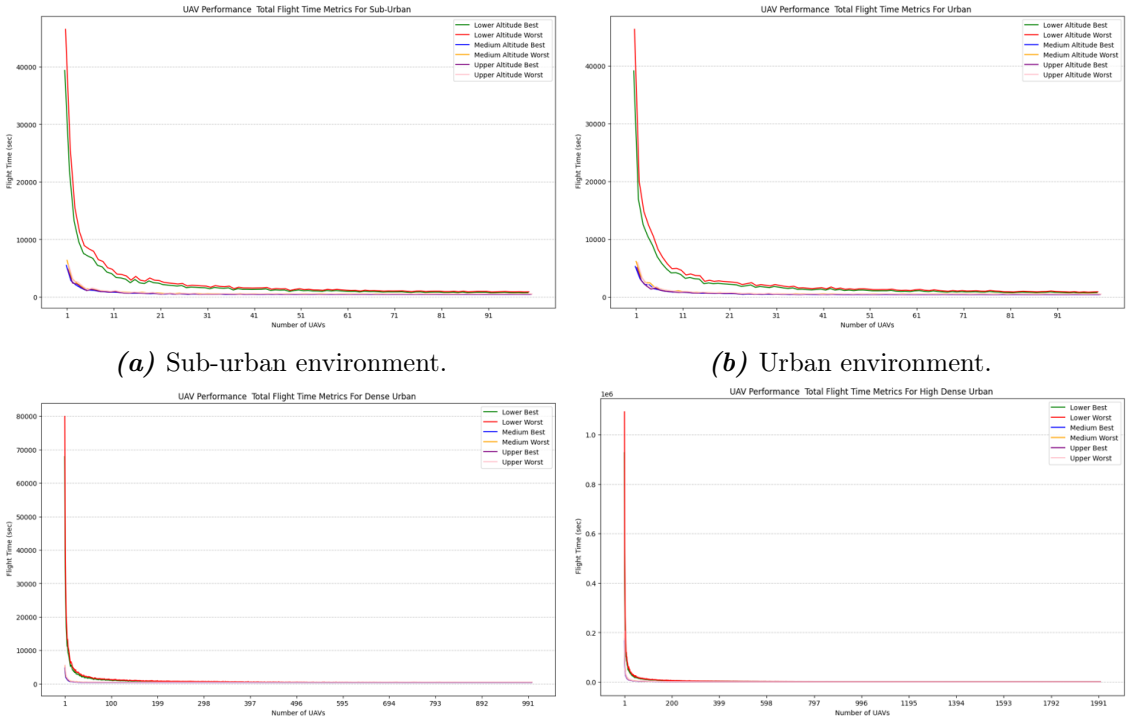

(a) Sub-urban environment.

(b) Urban environment.

(c) Dense-urban environment.

(d) Highrise-urban environment

Figure A.4. Performance analysis of RCI algorithm in different environment considerations in terms of total flight time to cover the target area.

A.2 IRCI Algorithm

Fig. A.5 shows the average total distance traveled by a single UAV of IRCI algorithm for lower, medium, and upper bound altitude in four different environments. The average total distance traveled is calculated by $\sum_{i=1}^{mn} dist_i$, where mn is the total waypoints and $dist_i$ is the distance between one waypoint to another waypoint. It can be seen that as the number of UAVs increases, the average distance traveled by a single UAV decreased. For all the environments, the average distance traveled by a single UAV for lower bound altitude is greater than other bound cases. Because in lower bound less number of UAVs are required to provide full coverage as compared to other bounds cases.

Fig. A.6 shows the average energy consumption of IRCI algorithm for lower, medium, and upper bound altitude in four different environments. The average energy consumption is calculated using Equation 3.6.12. It can be seen that in all the environments the energy consumption decreases with the increased number of UAVs because when the number of UAVs increases the flight time to cover the whole area decreases which results in decreased energy consumption. In Fig. A.6 (a), the medium bound cases have lower energy consumption compared to other bound cases. However, in other environments (b), (c), and (d), all the bound cases have no significant difference between energy consumption. This is due to the random movements of UAVs.

Fig. A.7 shows the average number of configurations of a single UAV of IRCI algorithm for different bound cases in all environments. The term configuration refer to the movement of UAV from one point to another. It can be seen that the average number of configurations

of single UAV decreases with increase in the number of UAVs. Because when the number of UAVs increases, the total configurations are divided between the UAVs, so the average number of configuration for single UAV decreases.

Fig. A.8 shows the average flight of a single UAV of IRCI algorithm for different bound cases in all environments. The average flight time ic calculated using Equation 3.6.7. It can be seen that as the number of UAVs increases, the average flight time of a single UAV decreased. For all the environments, the average distance traveled by a single UAV for lower bound altitude is greater than other bound cases. Because in lower bound less number of UAVs are required to provide full coverage as compared to other bounds cases.

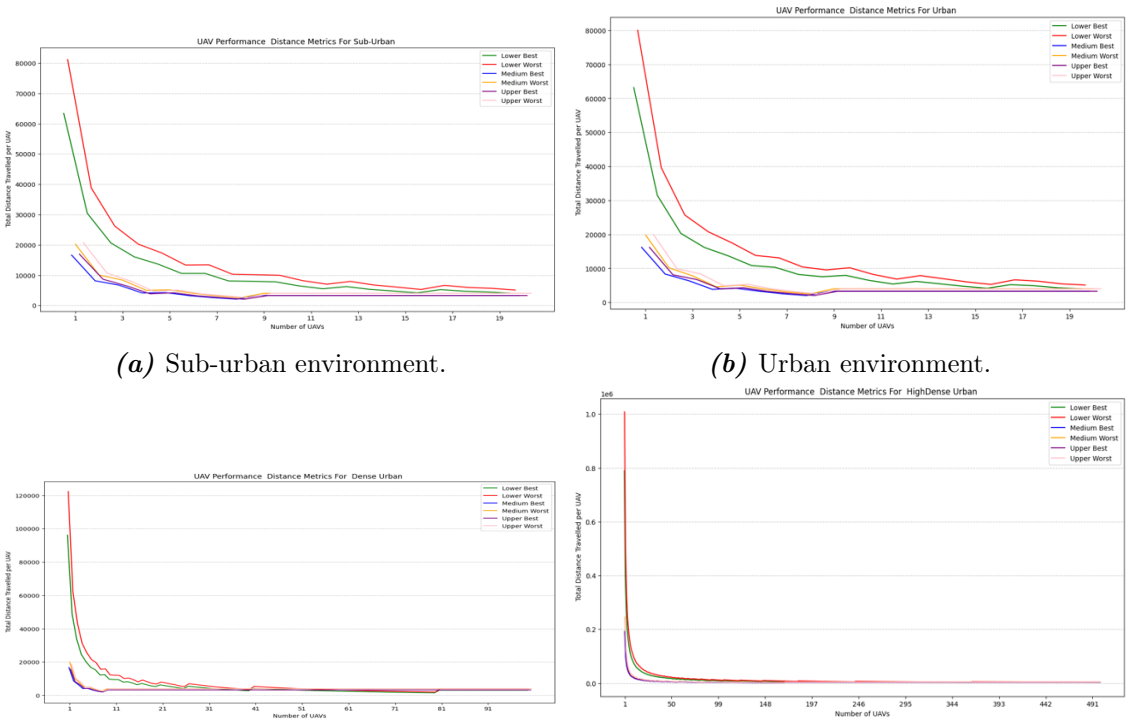

(a) Sub-urban environment.

(b) Urban environment.

(c) Dense-urban environment.

(d) Highrise-urban environment

Figure A.5. Performance analysis of IRCI algorithm in different environment considerations in terms of total distance traveled by UAVs to cover the target area.

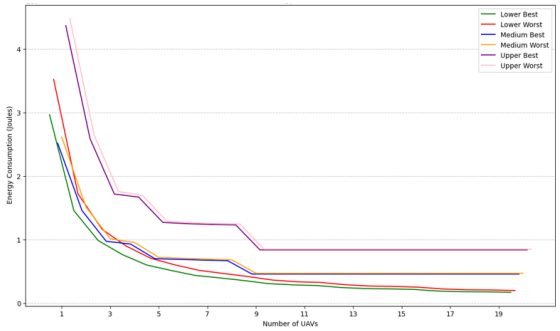

(a) Sub-urban environment. The scale of the y-axis for energy consumption is 10^6

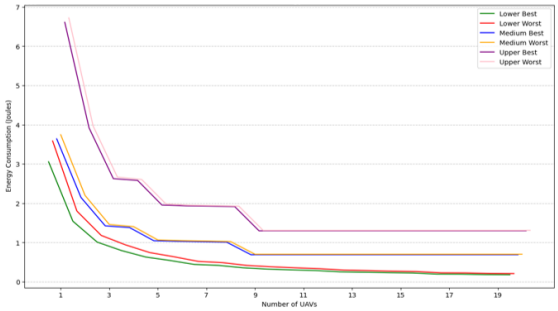

(b) Urban environment. The scale of the y-axis for energy consumption is 10^6

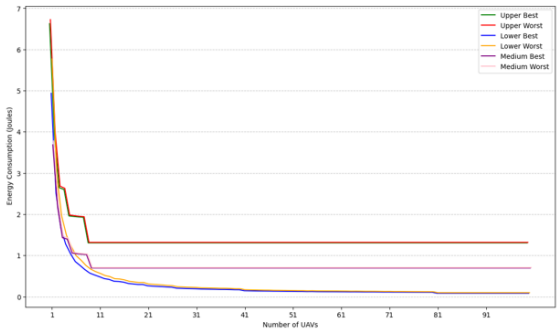

(c) Dense-urban environment. The scale of the y-axis for energy consumption is 10^6

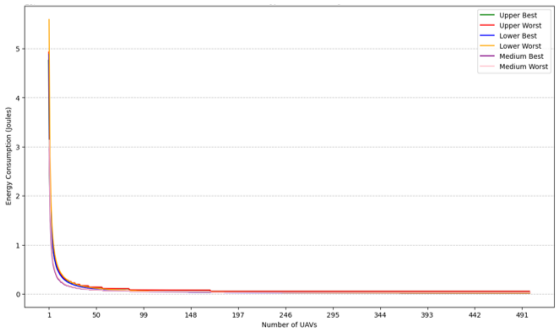

(d) Highrise-urban environment. The scale of the y-axis for energy consumption is 10^7

Figure A.6. Performance analysis of IRCI algorithm in different environment considerations in terms of energy consumption by UAVs to cover the target area.

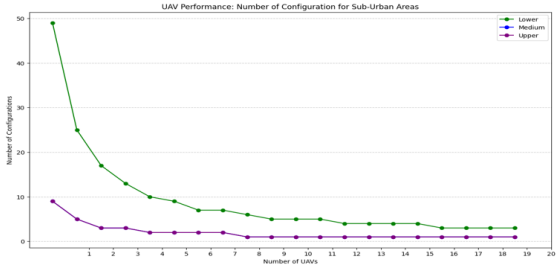

(a) Sub-urban environment.

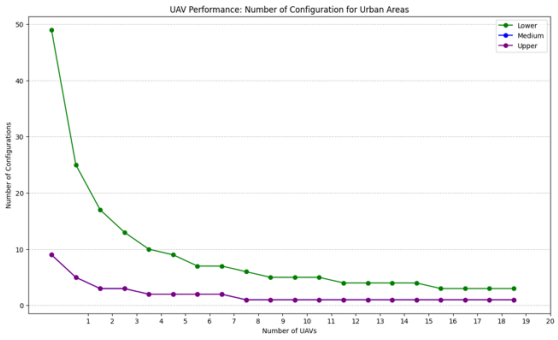

(b) Urban environment.

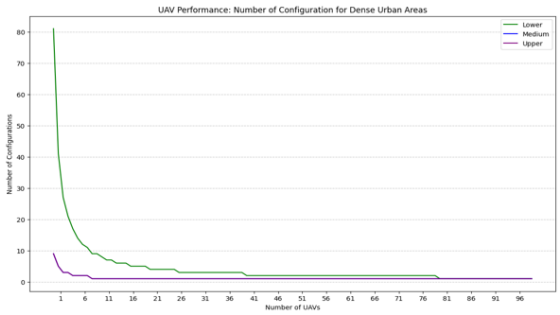

(c) Dense-urban environment.

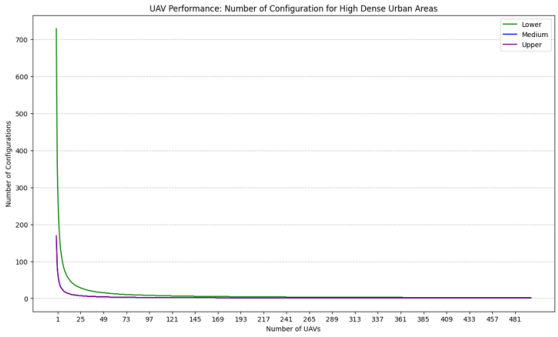

(d) Highrise-urban environment

Figure A.7. Performance analysis of IRCI in different environments in terms of number of configurations required to cover the target area.

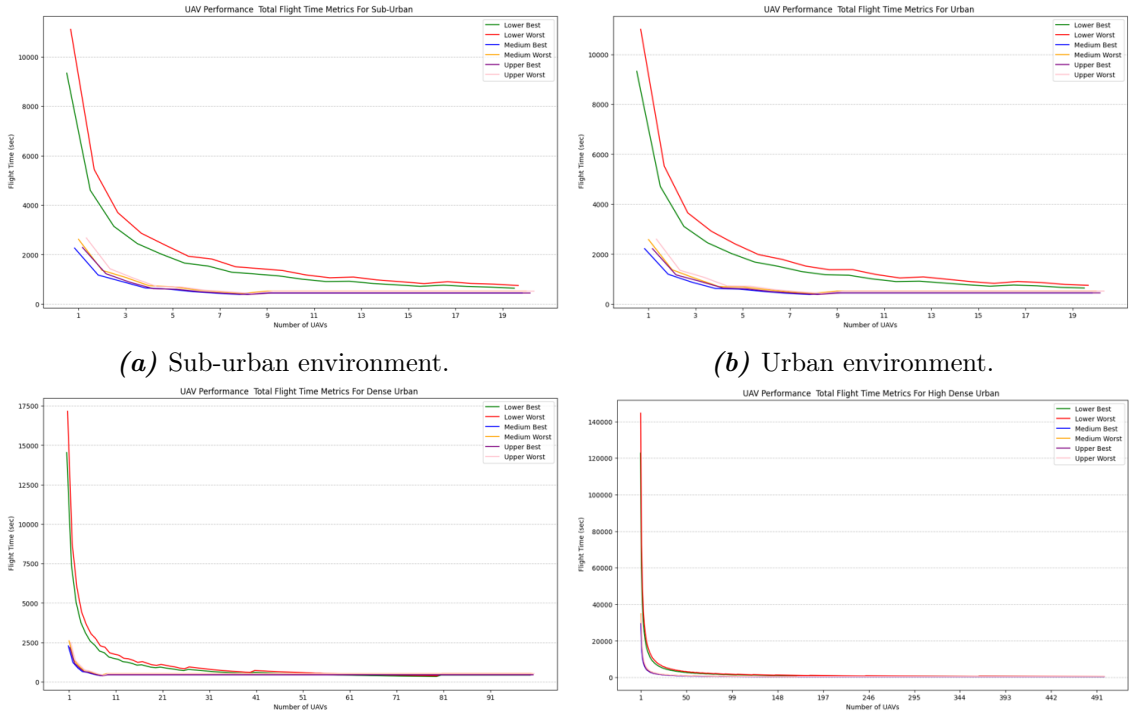

(a) Sub-urban environment.

(b) Urban environment.

(c) Dense-urban environment.

(d) Highrise-urban environment

Figure A.8. Performance analysis of IRCI algorithm in different environment considerations in terms of total flight time to cover the target area.

A.3 Scan Movement Algorithm

Fig. A.9 shows the average total distance traveled by a single UAV of scan movement algorithm for lower, medium, and upper bound altitude in four different environments. The average total distance traveled is calculated by $\sum_{i=1}^{mn} dist_i$, where mn is the total waypoints and $dist_i$ is the distance between one waypoint to another waypoint. It can be seen that as the number of UAVs increases, the average distance traveled by a single UAV decreased. For all the environments, the average distance traveled by a single UAV for lower bound altitude is greater than other bound cases. Because in lower bound less number of UAVs are required to provide full coverage as compared to other bounds cases.

Fig. A.10 shows the average energy consumption of scan movement algorithm for lower, medium, and upper bound altitude in four different environments. The average energy consumption is calculated using Equation 3.6.12. It can be seen that in all the environments the energy consumption decreases with the increased number of UAVs because when the number of UAVs increases the flight time to cover the whole area decreases which results in decreased energy consumption. In Fig. A.10 (a), (b), and (c), the lower bound cases have lower energy consumption compared to other bound cases. However, in A.10 (d) highrise-urban environment, all the bound cases have no significant difference in energy consumption as a significantly higher number of UAVs is required to cover the whole target area.

Fig. A.11 shows the average number of configurations of a single UAV of scan movement algorithm for different bound cases in all environments. The term configuration refer to the

movement of UAV from one point to another. It can be seen that the average number of configurations of single UAV decreases with increase in the number of UAVs. Because when the number of UAVs increases, the total configurations are divided between the UAVs, so the average number of configuration for single UAV decreases.

Fig. A.12 shows the average flight of a single UAV of scan movement algorithm for different bound cases in all environments. The average flight time ic calculated using Equation 3.6.7. It can be seen that as the number of UAVs increases, the average flight time of a single UAV decreased. For all the environments, the average distance traveled by a single UAV for lower bound altitude is greater than other bound cases. Because in lower bound less number of UAVs are required to provide full coverage as compared to other bounds cases.

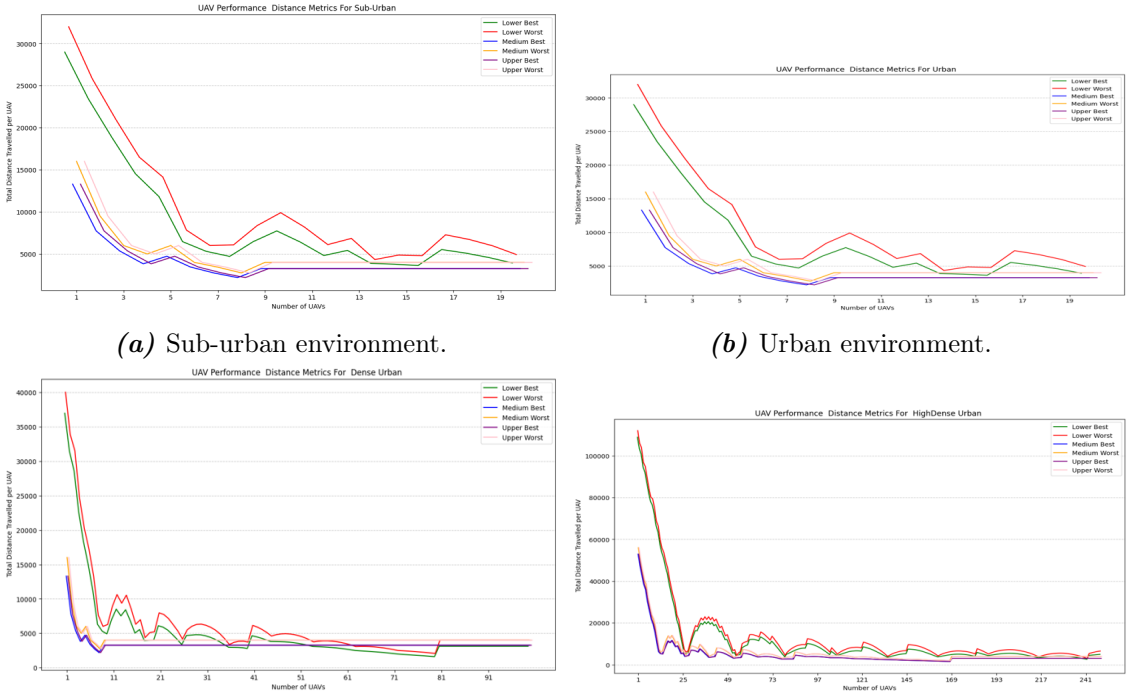

(a) Sub-urban environment.

(b) Urban environment.

(c) Dense-urban environment.

(d) Highrise-urban environment

Figure A.9. Performance analysis of scan movement algorithm in different environment considerations in terms of total distance traveled by UAVs to cover the target area.

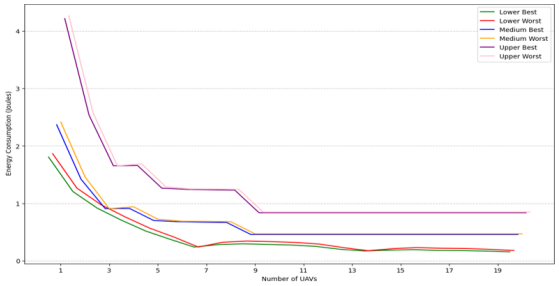

(a) Sub-urban environment.The scale of the y-axis for energy consumption is 10^6

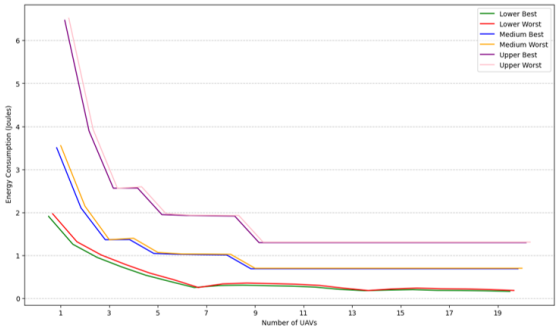

(b) Urban environment. The scale of the y-axis for energy consumption is 10^6

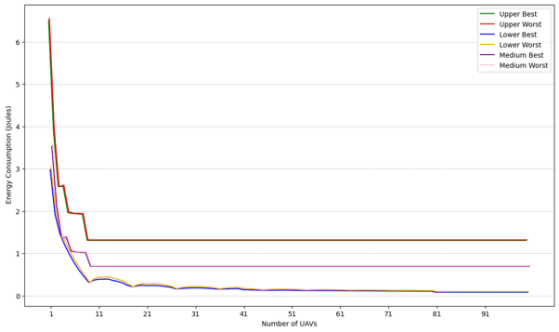

(c) Dense-urban environment. The scale of the y-axis for energy consumption is 10^6

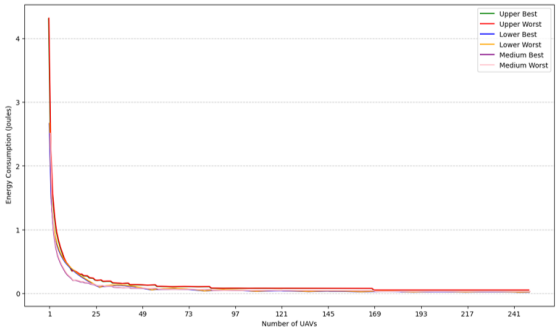

(d) Highrise-urban environment. The scale of the y-axis for energy consumption is 10^7

Figure A.10. Performance analysis of scan movement algorithm in different environment considerations in terms of energy consumption by UAVs to cover the target area.

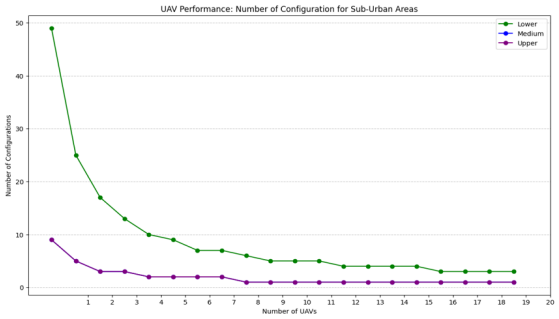

(a) Sub-urban environment.

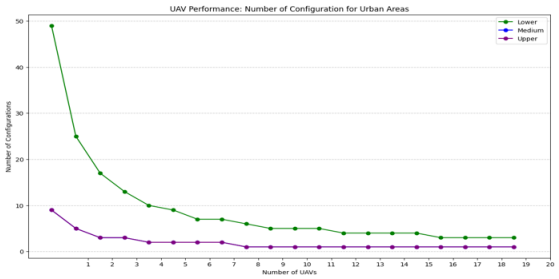

(b) Urban environment.

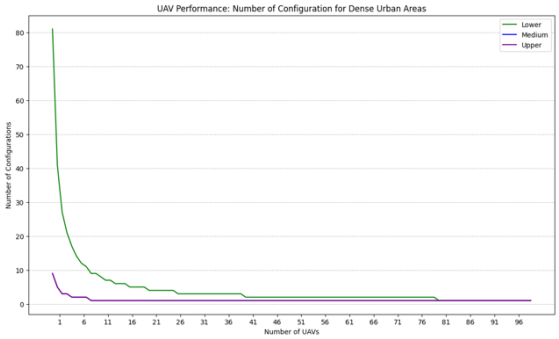

(c) Dense-urban environment.

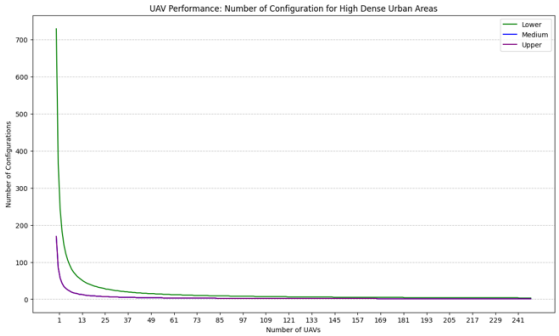

(d) Highrise-urban environment

Figure A.11. Performance analysis of scan movement in different environments considerations in terms of number of configurations required to cover the target area.

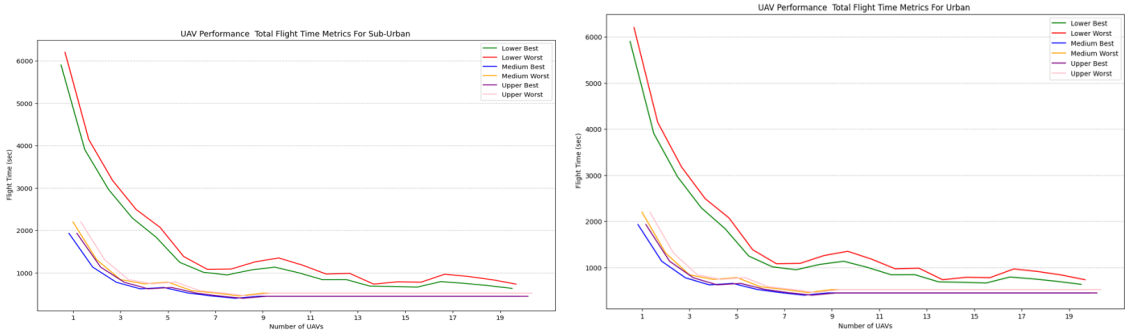

(a) Sub-urban environment.

(b) Urban environment.

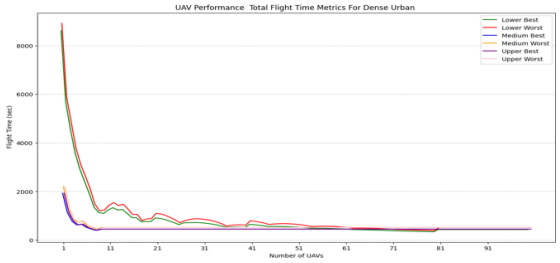

(c) Dense-urban environment.

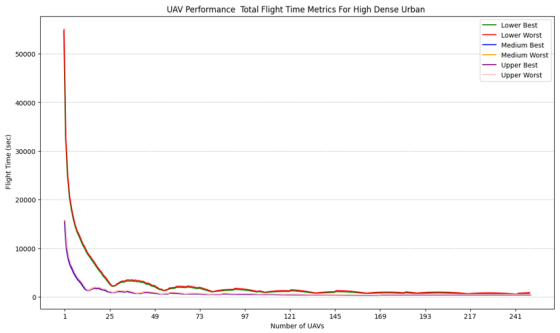

(d) Highrise-urban environment

Figure A.12. Performance analysis of scan movement algorithm in different environment considerations in terms of total flight time to cover the target area.

A.4 Nearest Movement Algorithm

Fig. A.13 shows the average total distance traveled by a single UAV of nearest movement algorithm for lower, medium, and upper bound altitude in four different environments. The average total distance traveled is calculated by $\sum_{i=1}^{mn} dist_i$, where mn is the total waypoints and $dist_i$ is the distance between one waypoint to another waypoint. It can be seen that as the number of UAVs increases, the average distance traveled by a single UAV decreased. For all the environments, the average distance traveled by a single UAV for lower bound altitude is greater than other bound cases. Because in lower bound less number of UAVs are required to provide full coverage as compared to other bounds cases.

Fig. A.14 shows the average energy consumption of nearest movement algorithm for lower, medium, and upper bound altitude in four different environments. The average energy consumption is calculated using Equation 3.6.12. It can be seen that in all the environments the energy consumption decreases with the increased number of UAVs because when the number of UAVs increases the flight time to cover the whole area decreases which results in decreased energy consumption. In Fig. A.14 (a), (b), and (c), the lower bound cases have lower energy consumption compared to other bound cases. However, in A.14 (d) highrise-urban environment, all the bound cases have no significant difference in energy consumption as a significantly higher number of UAVs is required to cover the whole target area.

Fig. A.15 shows the average number of configurations of a single UAV of nearest movement algorithm for different bound cases in all environments. The term configuration refer to the

movement of UAV from one point to another. It can be seen that the average number of configurations of single UAV decreases with increase in the number of UAVs. Because when the number of UAVs increases, the total configurations are divided between the UAVs, so the average number of configuration for single UAV decreases.

Fig. A.16 shows the average flight of a single UAV of nearest movement algorithm for different bound cases in all environments. The average flight time ic calculated using Equation 3.6.7. It can be seen that as the number of UAVs increases, the average flight time of a single UAV decreased. For all the environments, the average distance traveled by a single UAV for lower bound altitude is greater than other bound cases. Because in lower bound less number of UAVs are required to provide full coverage as compared to other bounds cases.

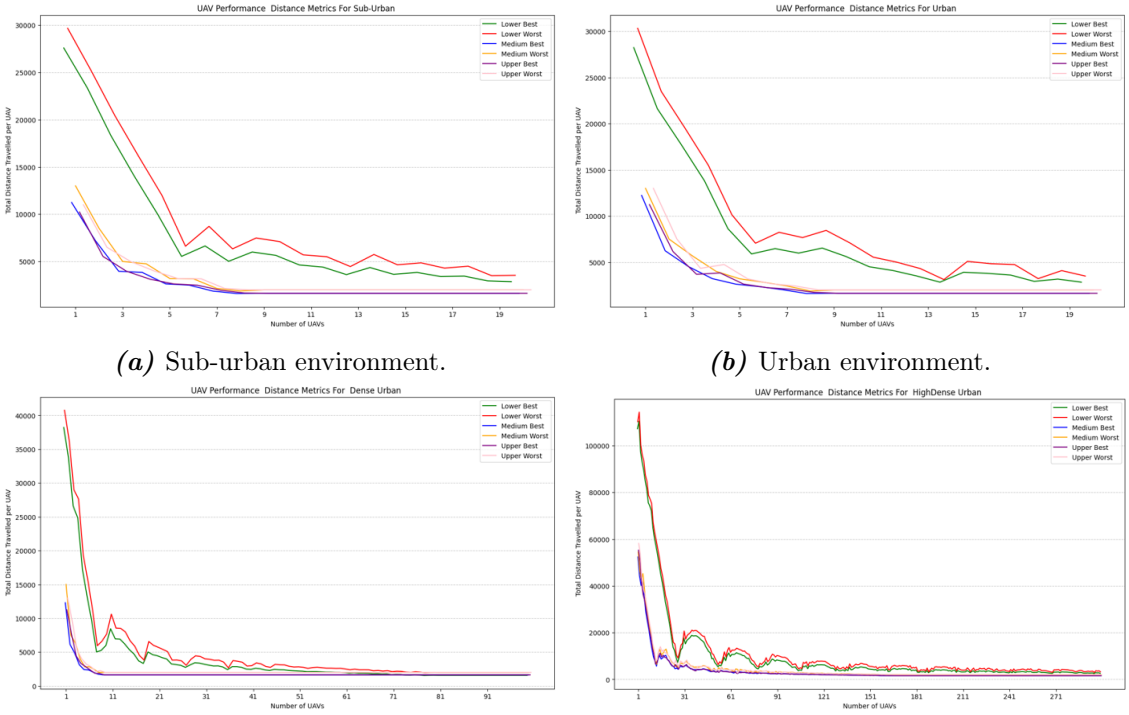

(a) Sub-urban environment.

(b) Urban environment.

(c) Dense-urban environment.

(d) Highrise-urban environment

Figure A.13. Performance analysis of nearest movement algorithm in different environment considerations in terms of total distance traveled by UAVs to cover the target area.

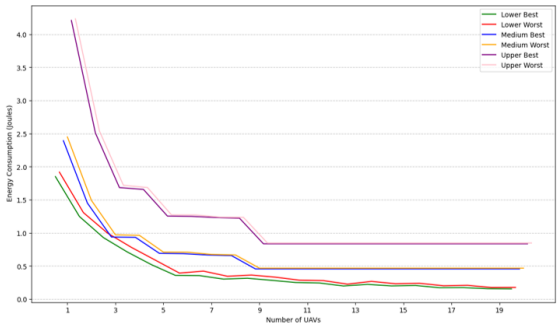

(a) Sub-urban environment. The scale of the y-axis for energy consumption is 10^6

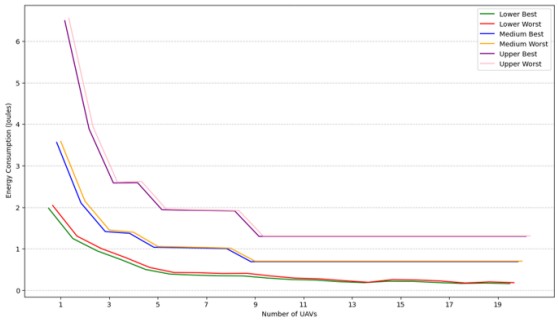

(b) Urban environment. The scale of the y-axis for energy consumption is 10^6

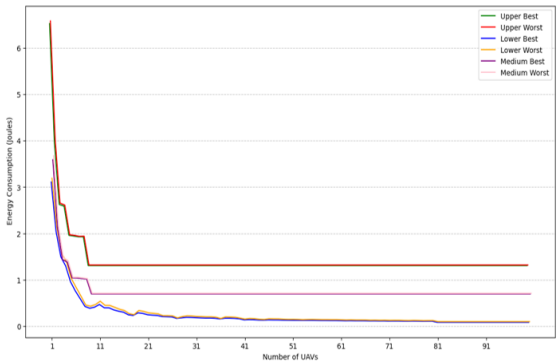

(c) Dense-urban environment. The scale of the y-axis for energy consumption is 10^6

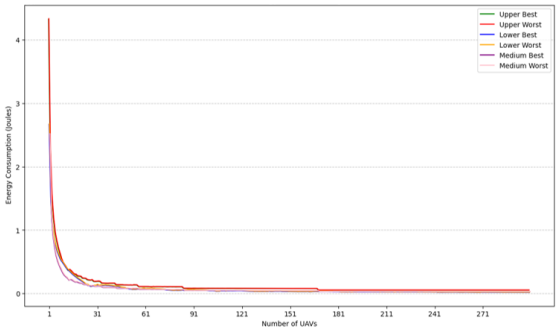

(d) Highrise-urban environment. The scale of the y-axis for energy consumption is 10^7

Figure A.14. Performance analysis of nearest movement algorithm in different environment considerations in terms of energy consumption by UAVs to cover the target area.

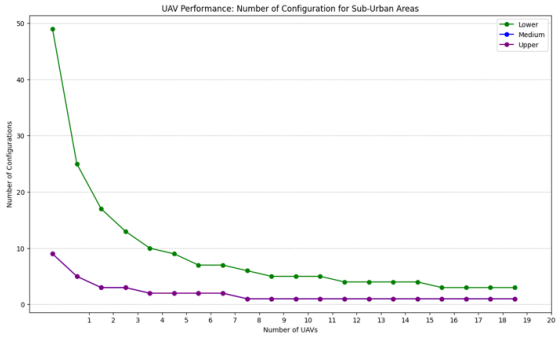

(a) Sub-urban environment.

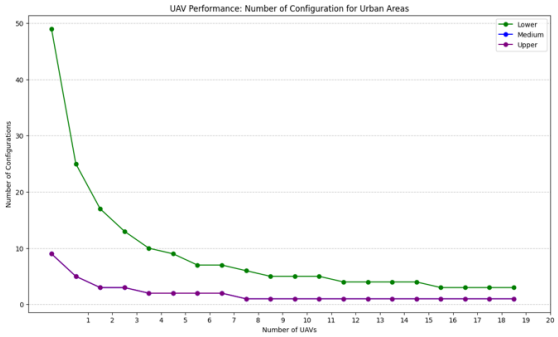

(b) Urban environment.

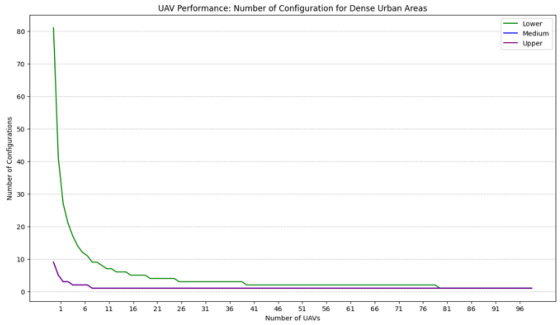

(c) Dense-urban environment.

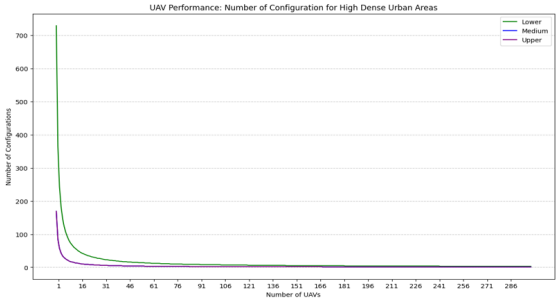

(d) Highrise-urban environment

Figure A.15. Performance analysis of nearest movement in different environment considerations in terms of number of configurations required to cover the target area.

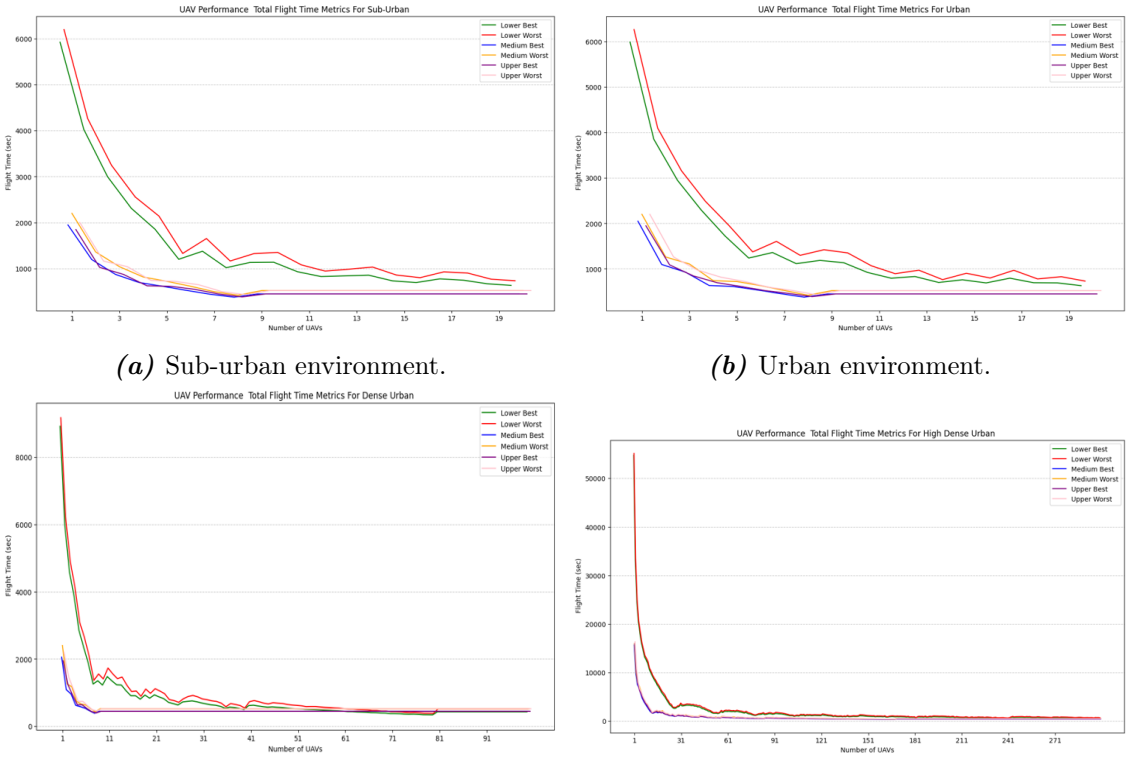

(a) Sub-urban environment.

(b) Urban environment.

(c) Dense-urban environment.

(d) Highrise-urban environment

Figure A.16. Performance analysis of nearest movement algorithm in different environment considerations in terms of total flight time to cover the target area.

A.4.1 Distance Formula

The two metrics for distance calculation are considered that are: Euclidean and Manhattan.

The Euclidean distance between two points (x_1, y_1) and (x_2, y_2) can be calculated as:

$$d_{Euc} = \sqrt{[(x_2 - x_1)^2 + (y_2 - y_1)^2]} \tag{A.4.1}$$

The Manhattan distance between two points (x_1, y_1) and (x_2, y_2) can be calculated as:

$$d_{Man} = |(x_2 - x_1)| + |(y_2 - y_1)| \tag{A.4.2}$$

Bibliography

Abeywickrama et al., **2018a**. Hasini Viranga Abeywickrama, Beeshanga Abewardana Jayawickrama, Ying He and Eryk Dutkiewicz. *Comprehensive Energy Consumption Model for Unmanned Aerial Vehicles, Based on Empirical Studies of Battery Performance.* IEEE Access, 6, 58383–58394, 2018a.

Abeywickrama et al., **2018b**. Hasini Viranga Abeywickrama, Beeshanga Abewardana Jayawickrama, Ying He and Eryk Dutkiewicz. *Comprehensive energy consumption model for unmanned aerial vehicles, based on empirical studies of battery performance.* IEEE access, 6, 58383–58394, 2018b.

Ahmed, **2023**. Amin Ahmed. *Asia-Pacific is world's most disaster-prone region.* `https://www.dawn.com/news/1730009`, 2023. [Online; accessed 30-Jan-2024].

Akram Al-Hourani, Sithamparanathan Kandeepan and Abbas Jamalipour, *2014a*. Akram Al-Hourani, Sithamparanathan Kandeepan and Abbas Jamalipour. Modeling air-to-ground path loss for low altitude platforms in urban environments. In *2014 IEEE Global Communications Conference*, pages 2898–2904, 2014a.

Al-Hourani et al., **2014b**. Akram Al-Hourani, Sithamparanathan Kandeepan and Simon Lardner. *Optimal LAP altitude for maximum coverage.* IEEE Wireless Communications Letters, 3(6), 569–572, 2014b.

Alzenad et al., **2017**. Mohamed Alzenad, Amr El-Keyi, Faraj Lagum and Halim Yanikomeroglu. *3-D placement of an unmanned aerial vehicle base station (UAV-BS) for energy-efficient maximal coverage.* IEEE Wireless Communications Letters, 6(4), 434–437, 2017.

Georgia E Athanasiadou and George V Tsoulos, *2019*. Georgia E Athanasiadou and George V Tsoulos. Path loss characteristics for UAV-to-ground wireless channels. In *2019 13th European Conference on Antennas and Propagation (EuCAP)*, pages 1–4. IEEE, 2019.

Beigi et al., **2022**. Pedram Beigi, Mohammad Sadra Rajabi and Sina Aghakhani. *An overview of drone energy consumption factors and models.* Handbook of Smart Energy Systems, pages 1–20, 2022.

Bi et al., **2023**. Suzhi Bi, Jiaxing Yu, Zheyuan Yang, Xiaohui Lin and Yuan Wu. *Joint 3D Deployment and Resource Allocation for UAV-assisted Integrated Communication and Localization.* IEEE Wireless Communications Letters, 2023.

Sridhar Bolli, *2020*. Sridhar Bolli. Propagation Path loss model based on Environmental Variables. In *2020 12th International Conference on Information Technology and Electrical Engineering (ICITEE)*, pages 368–373. IEEE, 2020.

R Irem Bor-Yaliniz, Amr El-Keyi and Halim Yanikomeroglu, 2016. R Irem Bor-Yaliniz, Amr El-Keyi and Halim Yanikomeroglu. Efficient 3-D placement of an aerial base station in next generation cellular networks. In *2016 IEEE international conference on communications (ICC)*, pages 1–5. IEEE, 2016.

Bose et al., 2022. Tushar Bose, Aala Suresh, Om Jee Pandey, Linga Reddy Cenkeramaddi and Rajesh M Hegde. *Improving quality-of-service in cluster-based UAV-assisted edge networks.* IEEE Transactions on Network and Service Management, 19(2), 1903–1919, 2022.

Dji, 2024. Dji. *Dji Camera Drones.* `https://www.dji.com/global/products/camera-drones`, 2024. [Online; accessed 13-Feb-2024].

Elmeseiry et al., 2021. Nourhan Elmeseiry, Nancy Alshaer and Tawfik Ismail. *A detailed survey and future directions of unmanned aerial vehicles (uavs) with potential applications.* Aerospace, 8(12), 363, 2021.

Góra et al., 2022. Krystian Góra, Paweł Smyczyński, Mateusz Kujawiński and Grzegorz Granosik. *Machine Learning in Creating Energy Consumption Model for UAV.* Energies, 15(18), 6810, 2022.

Huang and Savkin, 2022. Hailong Huang and Andrey V Savkin. *Deployment of heterogeneous UAV base stations for optimal quality of coverage.* IEEE Internet of Things Journal, 9(17), 16429–16437, 2022.

Javed et al., 2023. Sadaf Javed, Ali Hassan, Rizwan Ahmad, Waqas Ahmed, Muhammad Mahtab Alam and Joel JPC Rodrigues. *UAV trajectory planning for disaster scenarios.* Vehicular Communications, 39, 100568, 2023.

Kabashkin, 2023. Igor Kabashkin. *Availability of Services in Wireless Sensor Network with Aerial Base Station Placement.* Journal of Sensor and Actuator Networks, 12(3), 39, 2023.

Elham Kalantari, Halim Yanikomeroglu and Abbas Yongacoglu, 2016. Elham Kalantari, Halim Yanikomeroglu and Abbas Yongacoglu. On the number and 3D placement of drone base stations in wireless cellular networks. In *2016 IEEE 84th vehicular technology conference (VTC-Fall)*, pages 1–6. IEEE, 2016.

Khan et al., 2022. Amina Khan, Sumeet Gupta and Sachin Kumar Gupta. *Emerging UAV technology for disaster detection, mitigation, response, and preparedness.* Journal of Field Robotics, 39(6), 905–955, 2022.

Khawaja et al., 2020. Wahab Khawaja, Ozgur Ozdemir, Fatih Erden, Ismail Guvenc and David W Matolak. *Ultra-wideband air-to-ground propagation channel characterization in an open area.* IEEE transactions on aerospace and electronic systems, 56(6), 4533–4555, 2020.

Balaji Kirubakaran and Jiri Hosek, 2023. Balaji Kirubakaran and Jiri Hosek. Optimizing Tethered UAV Deployment for On-Demand Connectivity in Disaster Scenarios. In

2023 IEEE 97th Vehicular Technology Conference (VTC2023-Spring), pages 1–6. IEEE, 2023.

Kishk et al., **2020**. Mustafa Kishk, Ahmed Bader and Mohamed-Slim Alouini. *Aerial base station deployment in 6G cellular networks using tethered drones: The mobility and endurance tradeoff.* IEEE Vehicular Technology Magazine, 15(4), 103–111, 2020.

Lei et al., **2023**. Xing Lei, Xiaoxuan Hu, Guoqiang Wang and He Luo. *A multi-UAV deployment method for border patrolling based on Stackelberg game.* Journal of Systems Engineering and Electronics, 34(1), 99–116, 2023.

Li and Savkin, **2021**. Xiaohui Li and Andrey V Savkin. *Networked unmanned aerial vehicles for surveillance and monitoring: A survey.* Future Internet, 13(7), 174, 2021.

Liu et al., **2023**. Xiaojie Liu, Xingwei Wang, Min Huang, Jie Jia, Novella Bartolini, Qing Li and Dan Zhao. *Deployment of UAV-BSs for on-demand full communication coverage.* Ad Hoc Networks, 140, 103047, 2023.

Liu et al., **2022**. Yaxi Liu, Wei Huangfu, Huan Zhou, Haijun Zhang, Jiangchuan Liu and Keping Long. *Fair and energy-efficient coverage optimization for UAV placement problem in the cellular network.* IEEE Transactions on Communications, 70(6), 4222–4235, 2022.

Majeed et al., **2022**. Saqib Majeed, Adnan Sohail, Kashif Naseer Qureshi, Saleem Iqbal, Ibrahim Tariq Javed, Noel Crespi, Wamda Nagmeldin and Abdelzahir Abdelmaboud. *Coverage Area Decision Model by Using Unmanned Aerial Vehicles Base Stations for Ad Hoc Networks.* Sensors, 22(16), 6130, 2022.

Masroor et al., **2021**. Rooha Masroor, Muhammad Naeem and Waleed Ejaz. *Efficient deployment of UAVs for disaster management: A multi-criterion optimization approach.* Computer Communications, 177, 185–194, 2021.

Matolak and Sun, **2016**. David W Matolak and Ruoyu Sun. *Air–ground channel characterization for unmanned aircraft systems—Part I: Methods, measurements, and models for over-water settings.* IEEE Transactions on Vehicular Technology, 66(1), 26–44, 2016.

Mavroulis et al., **2019**. Spyridon Mavroulis, Emmanouil Andreadakis, Nafsika-Ioanna Spyrou, Varvara Antoniou, Emmanouel Skourtsos, Panayotis Papadimitriou, Ioannis Kasssaras, George Kaviris, Gerasimos-Akis Tselentis, Nikolaos Voulgaris et al. *UAV and GIS based rapid earthquake-induced building damage assessment and methodology for EMS-98 isoseismal map drawing: The June 12, 2017 Mw 6.3 Lesvos (Northeastern Aegean, Greece) earthquake.* International Journal of Disaster Risk Reduction, 37, 101169, 2019.

Xolani B Maxama and Elisha D Markus, *2018*. Xolani B Maxama and Elisha D Markus. A survey on propagation challenges in wireless communication networks over irregular terrains. In *2018 Open Innovations Conference (OI)*, pages 79–86. IEEE, 2018.

Mohsan et al., 2023. Syed Agha Hassnain Mohsan, Nawaf Qasem Hamood Othman, Yanlong Li, Mohammed H Alsharif and Muhammad Asghar Khan. *Unmanned aerial vehicles (UAVs): Practical aspects, applications, open challenges, security issues, and future trends.* Intelligent Service Robotics, 16(1), 109–137, 2023.

Moraitis et al., 2023. Nektarios Moraitis, Konstantinos Psychogios and Athanasios D Panagopoulos. *A Survey of Path Loss Prediction and Channel Models for Unmanned Aerial Systems for System-Level Simulations.* Sensors, 23(10), 4775, 2023.

Mohammad Mozaffari, Walid Saad, Mehdi Bennis and Merouane Debbah, 2015. Mohammad Mozaffari, Walid Saad, Mehdi Bennis and Merouane Debbah. Drone small cells in the clouds: Design, deployment and performance analysis. In *2015 IEEE global communications conference (GLOBECOM)*, pages 1–6. IEEE, 2015.

Mozaffari et al., 2016. Mohammad Mozaffari, Walid Saad, Mehdi Bennis and Mérouane Debbah. *Efficient deployment of multiple unmanned aerial vehicles for optimal wireless coverage.* IEEE Communications Letters, 20(8), 1647–1650, 2016.

Mozaffari et al., 2019. Mohammad Mozaffari, Walid Saad, Mehdi Bennis, Young-Han Nam and Mérouane Debbah. *A tutorial on UAVs for wireless networks: Applications, challenges, and open problems.* IEEE communications surveys & tutorials, 21(3), 2334–2360, 2019.

Munawar et al., 2022. Hafiz Suliman Munawar, Ahmed WA Hammad and S Travis Waller. *Disaster Region Coverage Using Drones: Maximum Area Coverage and Minimum Resource Utilisation.* Drones, 6(4), 96, 2022.

Naseem et al., 2018. Zahera Naseem, Iram Nausheen and Zahwa Mirza. *Propagation models for wireless communication system.* signal, 5(01), 2018.

Odesanya et al., 2023. Ituabhor Odesanya, Joseph Isabona, Emughedi Oghu and Okiemute Roberts Omasheye. *Hybrid Empirical and Machine Learning Approach to Efficient Path Loss Predictive Modelling: An Overview.* Int. J. Advanced Networking and Applications, 15(03), 5931–5939, 2023.

Pang et al., 2022. Minghui Pang, Qiuming Zhu, Cheng-Xiang Wang, Zhipeng Lin, Junyu Liu, Chongyu Lv and Zhuo Li. *Geometry-Based Stochastic Probability Models for the LoS and NLoS Paths of A2G Channels Under Urban Scenarios.* IEEE Internet of Things Journal, 10(3), 2360–2372, 2022.

Ranchagoda et al., 2021. Nirmani Hewa Ranchagoda, Kandeepan Sithamparanathan, Ming Ding, Akram Al-Hourani and Karina Mabell Gomez. *Elevation-angle based two-ray path loss model for Air-to-Ground wireless channels.* Vehicular Communications, 32, 100393, 2021.

Sabzehali et al., 2022. Javad Sabzehali, Vijay K Shah, Qiang Fan, Biplav Choudhury, Lingjia Liu and Jeffrey H Reed. *Optimizing number, placement, and backhaul connectivity of multi-UAV networks.* IEEE Internet of Things Journal, 9(21), 21548–21560, 2022.

Saif et al., **2021**. Abdu Saif, Kaharudin Dimyati, Kamarul Ariffin Noordin, Nor Shahida Mohd Shah, Qazwan Abdullah, Mahathir Mohamad, Mahmod Abd Hakim Mohamad and Ahmed M Al-Saman. *Unmanned aerial vehicle and optimal relay for extending coverage in post-disaster scenarios.* arXiv preprint arXiv:2104.06037, 2021.

Salas, **2024a**. Erick Burgueño Salas. *Economic losses from natural disaster events worldwide from 2000 to 2023.* `https://www.statista.com/statistics/510894/natural-disasters-globally-and-economic-losses/#:~:text=Global%20economic%20losses%20from%20natural%20disasters%202000%2D2023&text=In%202023%2C%20the%20economic%20losses,of%20natural%20processes%20on%20Earth.`, 2024a. [Online; accessed 25-Feb-2024].

Salas, **2024b**. Erick Burgueño Salas. *Number of deaths from natural disaster events worldwide from 2000 to 2023.* `https://www.statista.com/statistics/510952/number-of-deaths-from-natural-disasters-globally/`, 2024b. [Online; accessed 25-Feb-2024].

Salas, **2023**. Erick Burgueño Salas. *Number of natural disaster events worldwide from 2000 to 2022.* `https://www.statista.com/statistics/510959/number-of-natural-disasters-events-globally/`, 2023. [Online; accessed 10-Jan-2024].

Sami et al., **2023**. Hani Sami, Reem Saado, Ahmad El Saoudi, Azzam Mourad, Hadi Otrok and Jamal Bentahar. *Opportunistic UAV Deployment for Intelligent On-Demand IoV Service Management.* IEEE Transactions on Network and Service Management, 2023.

Seraj et al., **2022**. Esmaeil Seraj, Andrew Silva and Matthew Gombolay. *Multi-UAV planning for cooperative wildfire coverage and tracking with quality-of-service guarantees.* Autonomous Agents and Multi-Agent Systems, 36(2), 39, 2022.

Sharafeddine and Islambouli, **2019**. Sanaa Sharafeddine and Rania Islambouli. *On-demand deployment of multiple aerial base stations for traffic offloading and network recovery.* Computer Networks, 156, 52–61, 2019.

Su et al., **2023**. Yuhan Su, Minghui Liwang, Zhong Chen and Xiaojiang Du. *Toward Optimal Deployment of UAV Relays in UAV-Assisted IoV Networks.* IEEE Transactions on Vehicular Technology, 2023.

Sun et al., **2022**. Yutong Sun, Jianhua Zhang, Yuxiang Zhang, Li Yu, Zhiqiang Yuan, Guangyi Liu and Qixing Wang. *Environment features-based model for path loss prediction.* IEEE Wireless Communications Letters, 11(9), 2010–2014, 2022.

Van Huynh et al., **2021**. Dang Van Huynh, Tan Do-Duy, Long D Nguyen, Minh-Tuan Le, Nguyen-Son Vo and Trung Q Duong. *Real-time optimized path planning and energy consumption for data collection in unmanned ariel vehicles-aided intelligent wireless sensing.* IEEE Transactions on Industrial Informatics, 18(4), 2753–2761, 2021.

Viet and Romero, **2022**. Pham Q Viet and Daniel Romero. *Aerial base station placement: A tutorial introduction.* IEEE Communications Magazine, 60(5), 44–49, 2022.

Zhe Wang, Lingjie Duan and Rui Zhang, 2018. Zhe Wang, Lingjie Duan and Rui Zhang. Traffic-aware adaptive deployment for UAV-aided communication networks. In *2018 IEEE Global Communications Conference (GLOBECOM)*, pages 1–6. IEEE, 2018.

Wu et al., 2023. Kefeng Wu, Kwan-Wu Chin and Sieteng Soh. *UAVs Deployment Algorithms for Maximizing Backhaul Flow.* IEEE Systems Journal, 2023.

Zhang et al., 2021. Juan Zhang, James F Campbell, Donald C Sweeney II and Andrea C Hupman. *Energy consumption models for delivery drones: A comparison and assessment.* Transportation Research Part D: Transport and Environment, 90, 102668, 2021.

Zhao et al., 2019. Nan Zhao, Weidang Lu, Min Sheng, Yunfei Chen, Jie Tang, F Richard Yu and Kai-Kit Wong. *UAV-assisted emergency networks in disasters.* IEEE Wireless Communications, 26(1), 45–51, 2019.

Zhu and Zhou, 2023. Xiaojian Zhu and MengChu Zhou. *Maximal Weighted Coverage Deployment of UAV-Enabled Rechargeable Visual Sensor Networks.* IEEE Transactions on Intelligent Transportation Systems, 2023.